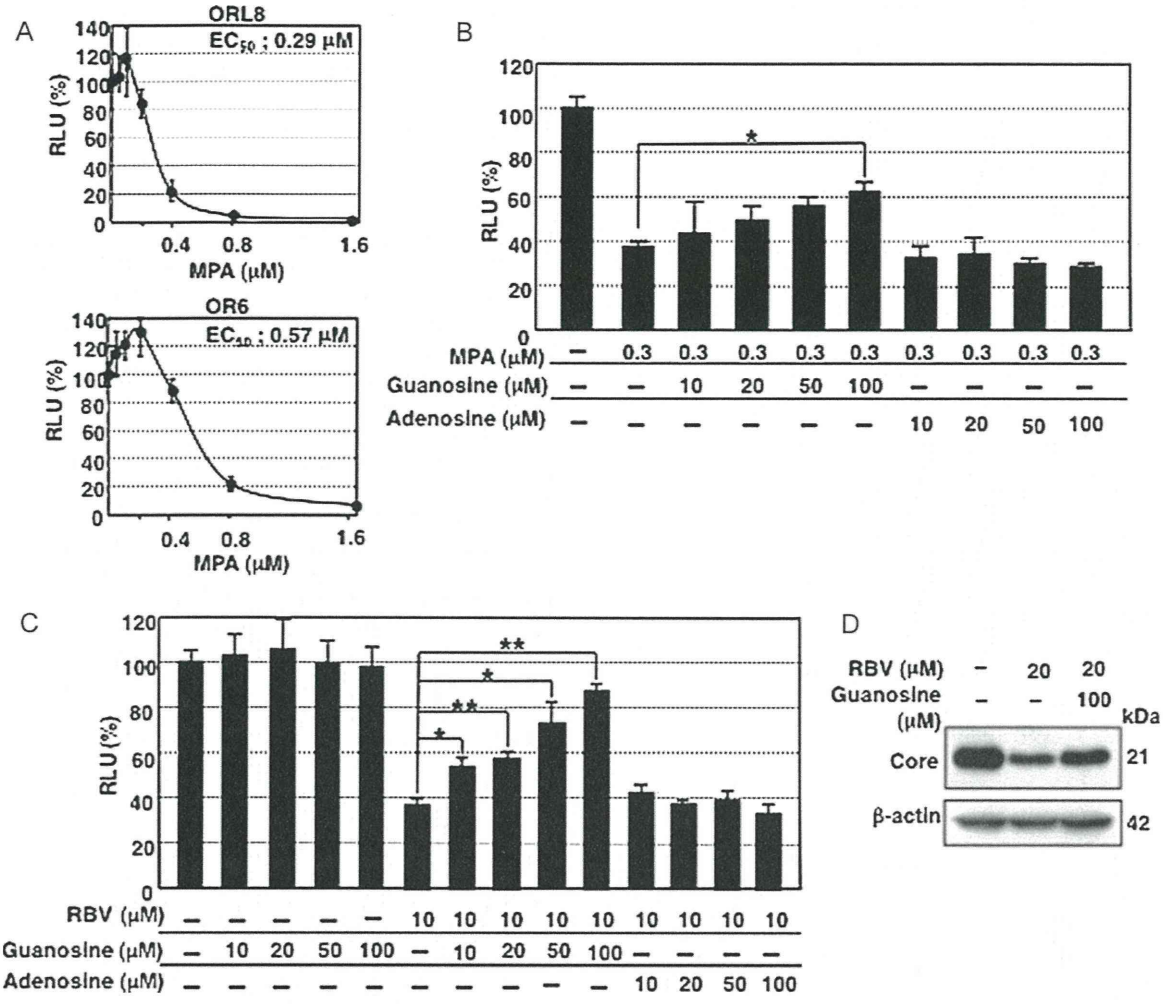

Fig. 6. Guanosine canceled the anti-HCV activity of RBV in ORL8 system. (A) Anti-HCV activity of MPA in ORL8 and OR6. The ORL8 and OR6 cells were treated with MPA for 72 h, and then RL assay was performed. (B) Effect of guanosine or adenosine on MPA in ORL8 system. ORL8 cells were treated with MPA alone or in combination with guanosine or adenosine for 72 h, and then RL assay was performed. Asterisk indicates a significant difference compared to the control treatment. $^{*}P < 0.05$. (C) Effect of guanosine or adenosine on RBV in ORL8 system. ORL8 cells were treated with RBV alone or in combination with guanosine or adenosine for 72 h, and then the RL assay was performed. Asterisks indicate significant differences compared to the control treatment. $^{*}P < 0.05$; $^{**}P < 0.01$. (D) Effect of guanosine on RBV in ORL8 system. ORL8 cells were treated with RBV alone or in combination with guanosine for 72 h, and subjected to Western blot analysis using anti-Core and β-actin antibodies.

et al., 2002; Thomas et al., 2011; Zhou et al., 2003). Although the effective concentrations (50–1000 μM) of RBV in those studies were much higher than the clinically achievable concentrations (5–14 μM) (Feld et al., 2010; Pawlotsky et al., 2004; Tanabe et al., 2004), the effective concentration of RBV in this study was close to the clinically achievable concentrations. Furthermore, it is noteworthy that the replication of a different HCV strain (JFH1 of genotype 2a) in the Li23-derived cell culture system, but not in the HuH-7-derived cell culture system, was also suppressed with RBV at the concentration of 10 μM (Fig. 1C). These results demonstrate that the Li23 cell-derived assay system is a more sensitive biosensor of RBV than the HuH-7 cell-derived assay system.

The finding that RBV remarkably inhibited HCV RNA replication in our new assay systems led us to analyze the anti-HCV mechanism of RBV. In this study, we evaluated several possible anti-HCV mechanisms of RBV, as described above. Regarding the induction of error catastrophe by RBV, we obtained no evidence that RBV (even at 50 μM) acted as a mutagen in HCV RNA replication. Therefore, we could not explain the mechanism underlying the suppression of HCV RNA replication by RBV according to the theory of error catastrophe. In addition, no increasing mutation rate of HCV RNA in patients receiving RBV monotherapy or a combination of RBV plus IFN-α was observed in a previous clinical study (Chevaliez and Pawlotsky, 2007). In consideration of all these findings, we suggest that the clinically achievable concentrations of RBV do not act as a mutagen in HCV RNA replication. Indeed, our previous study using the replicon cell culture system demonstrated that RBV treatment (6 months at 5 and 25 μM) did not accelerate the mutation rate or increase the genetic diversity of the HCV replicon (Kato et al., 2005). In regard to the effect of RBV on the IFN system, we obtained no evidence that RBV (even at 50 μM) induced ISGs (ISG15, IRF7, and IP-10) or phosphorylation of STAT1 even in the cells co-treated with IFN-α and RBV (data not shown). On the other hand, very recently Thomas et al. (Thomas et al., 2011) reported that RBV treatment (500 μM) resulted in the induction of a distinct set of ISGs including ISG15, IRF7, and IRF9, using HuH-7-derived cell line Huh7.5.1. In that study, they demonstrated that the induction of these ISGs was mediated by a novel mechanism different from those associated with IFN signaling and double stranded RNA sensing pathway, and concluded that the effect of RBV on ISG regulation is IFN-independent. However, in our cell culture system, which is highly sensitive to RBV, the induction of ISG15 and IRF7 by RBV was not observed (Fig. 4C). This kind of controversial results may be dependent on the difference of cell lines used in both studies, since recent microarray analysis revealed that the expression profiles of Li23 and HuH-7 cells, both of which possess an environment

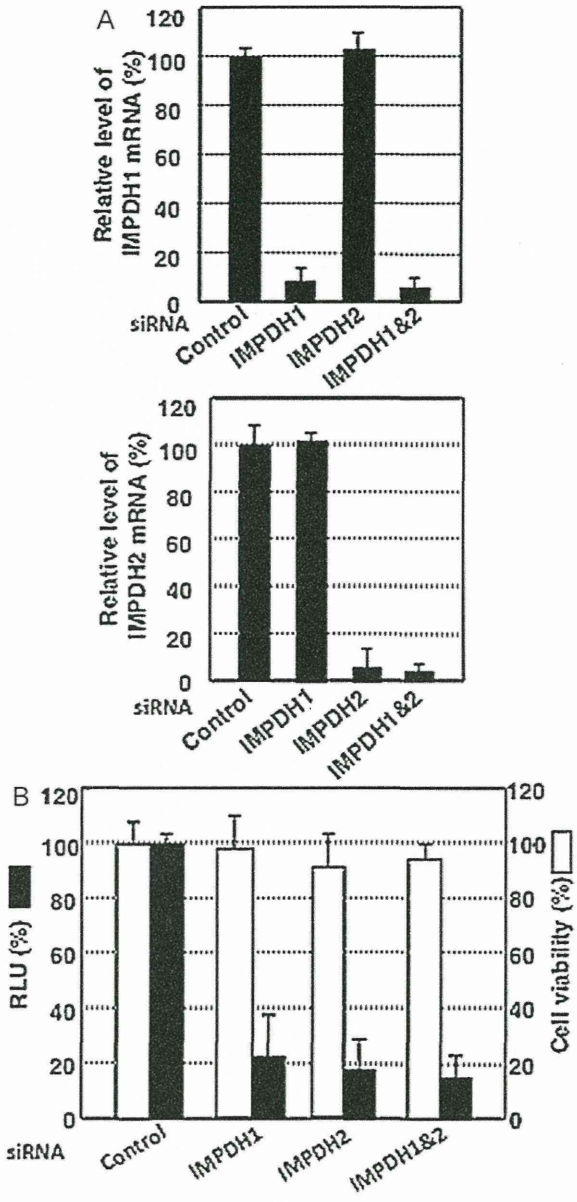

Fig. 7. IMPDH is required for HCV RNA replication. (A) Inhibition of IMPDH1 and IMPDH2 expression by siRNA in ORL8 cells. ORL8 cells were transfected with 8 nM siRNA targeting for IMPDH1 and/or IMPDH2. After 72 h, the expression levels of IMPDH1 and IMPDH2 mRNAs were determined by the quantitative RT-PCR. Experiments were done in triplicate. (B) Suppression of HCV RNA replication in IMPDH1- and/or IMPDH2-knockdown ORL8 cells. The RLU (%) calculated, when the luciferase activity of the cells treated with control siRNA was assigned to be 100%, is shown. The cell viability was determined as described in Section 2.

for robust HCV replication, differed considerably (Kato et al., 2009; Mori et al., 2010). However, Thomas et al. (2011) observed that the addition of guanosine to the medium could block RBV-induced ISGs induction. Therefore, further additional studies would be needed to resolve the differences of results obtained from both studies.

The highlight in this study is that a Li23-derived cell culture system clearly demonstrated an association between the suppression of HCV RNA replication by RBV and IMPDH inhibition by RBV. Although RBV is known to be an IMPDH inhibitor (Lau et al., 2002), it had been considered that such inhibitory activity would not contribute to the anti-HCV activity of RBV, because of the marginal antiviral effect of RBV in HuH-7-derived HCV RNA replicating cells (Naka et al., 2005; Tanabe et al., 2004; Zhou et al., 2003). Although Zhou et al. (2003) previously showed that exogenous guanosine cancelled the RBV-induced CFE reduction using an HuH-7-based HCV replicon system, they did not observe any dose-dependent reversion of the adverse effect of RBV by the addition of guanosine. However, in our Li23-based HCV replication assay system, we observed a near complete cancellation of the activity of RBV in the dose-dependent manner of guanosine (Fig. 6C). This finding indicated that anti-HCV activity of RBV might be mediated through the inhibition of IMPDH by RBV. Indeed, we could demonstrate that HCV RNA replication was notably suppressed in IMPDH-knockdown ORL8 cells (Fig. 7B). Taken together, these results revealed that the Li23-derived assay system was superior to HuH-7-derived assay system in order to clarify the anti-HCV mechanism of RBV.

The remarkable effect of RBV observed in this study was considered to be due to the difference in the cell lines used, because Li23-derived cells possessed rather different gene expression profiles from those in HuH-7-derived cells (Kato et al., 2009; Mori et al., 2010). As one of the possibilities, we examined the expression status of nucleoside transporters (ENT family) involved in cellular uptake of RBV or ATP-binding cassette transporters, including multidrug resistance 1, which is involved in cellular excretion. However, the mRNA levels of these transporters were almost the same in both types of cells (Fig. 3C). Although unfortunately we failed to clarify the mechanism underlying the remarkable differences in the activity of RBV in both types of cells, we observed that the anti-HCV activity of RBV was completely canceled by NBMPR, an ENT inhibitor, suggesting that RBV is taken by ENT member(s) at least in ORL8 cells. This finding supports the recent report describing the involvement of ENT1 on cellular uptake of RBV (Fukuchi et al., 2010; Ibarra and Pfeiffer, 2009). Therefore, a comparative analysis regarding the functions of ENT member(s) derived from both types of cells will be needed. As the other possibility, the differences of activities or expression levels of IMPDH in OR6 and ORL8 cells may contribute to the remarkable effect of RBV observed in ORL8 cells.

On the other hand, it has been known that rapid reduction of the intracellular level of GTP occurs when RBV inhibits IMPDH (Feld and Hoofnagle, 2005). Therefore, it is assumed that the decrease of GTP would lead to a suppression of HCV replication. To date, several studies (Lohmann et al., 1999; Luo et al., 2000; Simister et al., 2009) have shown that high concentration of GTP (approximately 500 μM corresponding to the intracellular concentration) is required for the efficient de novo initiation of RNA synthesis by HCV NS5B RdRp. In addition, Simister et al. (2009) showed that change from 500 μM to 100 μM of GTP concentration decreased a log of the NS5B RdRp activity. From these studies, we expect that the inhibition of IMPDH by RBV may cause rapid decrease of intracellular GTP concentration, resulting in the suppression of de novo RNA synthesis by NS5B. Before our assumption, MMPD/VX-497 has developed as an inhibitor of IMPDH, and it has been shown to exert anti-HCV activity (EC_{50}; 0.39 μM) in an HCV replicon system (Marcellin et al., 2007). However, MMPD/VX-497 monotherapy of patients with chronic hepatitis C had no effect on HCV RNA levels (Marcellin et al., 2007) just as, in another study, RBV monotherapy had no effect on HCV RNA levels in patients with chronic hepatitis C (Di Bisceglie et al., 1995). Although we showed that the EC_{50} value of RBV in this study was equivalent to the clinically achievable concentrations (Feld et al., 2010; Pawlotsky et al., 2004; Tanabe et al., 2004), we considered that the effective concentration for a reduction of HCV RNA levels in monotherapy would be less than the EC_{90} value. However, an IMPDH inhibitor at EC_{50} would be effective in combination with IFN-α as an adjuvant. Indeed, combination therapy with IFN-α and MMPD/VX-497 was effective in previously untreated patients with chronic hepatitis C (McHutchison et al., 2005). However, a recent study (Rustgi et al., 2009) showed that the addition of MMPD/VX-497 to PEG-IFN-α and RBV combination

therapy in patients who had been nonrespondent to PEG-IFN-α and RBV combination therapy did not increase the proportion of patients who achieved an SVR. Since we showed that RBV also acted as an IMPDH inhibitor in the present study, it would seem to be a reasonable result that MMPD/VX-497 had no significant effect on patients who were nonresponsive to combination therapy with PEG-IFN-α and RBV.

In conclusion, we clarified the anti-HCV mechanism of RBV in a new HCV cell culture system. The fact that anti-HCV activity of RBV was mediated by the inhibition of IMPDH would provide a clue to the mechanism of the increase of SVR by the current standard combination therapy with PEG-IFN-α and RBV. In addition, our findings should also be useful for the screening and development of new anti-HCV drugs, which inhibit IMPDH, with reduced side effects, including anemia.

Acknowledgments

We would like to thank Naoko Kawahara, Takashi Nakamura, and Keiko Takeshita for their technical assistances. This work was supported by a grant-in-aid for research on hepatitis from the Ministry of Health, Labor, and Welfare of Japan. K. M. was supported by a Research Fellowship from the Japan Society for Promotion of Science for Young Scientists.

References

Ariumi, Y., Kuroki, M., Abe, K., Dansako, H., Ikeda, M., Wakita, T., Kato, N., 2007. DDX3 DEAD-box RNA helicase is required for hepatitis C virus RNA replication. J. Virol. 81, 13922–13926.

Chevaliez, S., Brillet, R., Lázaro, E., Hézode, C., Pawlotsky, J.M., 2007. Analysis of ribavirin mutagenicity in human hepatitis C virus infection. J. Virol. 81, 7732–7741.

Chevaliez, S., Pawlotsky, J.M., 2007. Interferon-based therapy of hepatitis C. Adv. Drug. Deliv. Rev. 59, 1222–1241.

Contreras, A.M., Hiasa, Y., He, W., Terella, A., Schmidt, E.V., Chung, R.T., 2002. Viral RNA mutations are region specific and increased by ribavirin in a full-length hepatitis C virus replication system. J. Virol. 76, 8505–8517.

Dansako, H., Ikeda, M., Kato, N., 2007. Limited suppression of the interferon-beta production by hepatitis C virus serine protease in cultured human hepatocytes. FEBS J. 274, 4161–4176.

Dansako, H., Naganuma, A., Nakamura, T., Ikeda, F., Nozaki, A., Kato, N., 2003. Differential activation of interferon-inducible genes by hepatitis C virus core protein mediated by the interferon stimulated response element. Virus Res. 97, 17–30.

Di Bisceglie, A.M., Conjeevaram, H.S., Fried, M.W., Sallie, R., Park, Y., Yurdaydin, C., Swain, M., Kleiner, D.E., Mahaney, K., Hoofnagle, J.H., 1995. Ribavirin as therapy for chronic hepatitis C. A randomized, double-blind, placebo-controlled trial. Ann. Intern. Med. 123, 897–903.

Feld, J.J., Lutchman, G.A., Heller, T., Hara, K., Pfeiffer, J.K., Leff, R.D., Meek, C., Rivera, M., Ko, M., Koh, C., Rotman, Y., Ghany, M.G., Haynes-Williams, V., Neumann, A.U., Liang, T.J., Hoofnagle, J.H., 2010. Ribavirin improves early responses to peginterferon through improved interferon signaling. Gastroenterology 139, 154–162.

Feld, J.J., Hoofnagle, J.H., 2005. Mechanism of action of interferon and ribavirin in treatment of hepatitis C. Nature 436, 967–972.

Fukuchi, Y., Furihata, T., Hashizume, M., Iikura, M., Chiba, K., 2010. Characterization of ribavirin uptake systems in human hepatocytes. J. Hepatol. 52, 486–492.

Henry, S.D., Metselaar, H.J., Lonsdale, R.C., Kok, A., Haagmans, B.L., Tilanus, H.W., van der Laan, L.J., 2006. Mycophenolic acid inhibits hepatitis C virus replication and acts in synergy with cyclosporin A and interferon-alpha. Gastroenterology 131, 1452–1462.

Ibarra, K.D., Pfeiffer, J.K., 2009. Reduced ribavirin antiviral efficacy via nucleoside transporter-mediated drug resistance. J. Virol. 83, 4538–4547.

Ikeda, M., Abe, K., Dansako, H., Nakamura, T., Naka, K., Kato, N., 2005. Efficient replication of a full-length hepatitis C virus genome, strain O, in cell culture, and development of a luciferase reporter system. Biochem. Biophys. Res. Commun. 329, 1350–1359.

Kato, N., Hijikata, M., Ootsuyama, Y., Nakagawa, M., Ohkoshi, S., Sugimura, T., Shimotohno, K., 1990. Molecular cloning of the human hepatitis C virus genome from Japanese patients with non-A, non-B hepatitis. Proc. Natl. Acad. Sci. U.S.A. 87, 9524–9528.

Kato, N., Mori, K., Abe, K., Dansako, H., Kuroki, M., Ariumi, Y., Wakita, T., Ikeda, M., 2009. Efficient replication systems for hepatitis C virus using a new human hepatoma cell line. Virus Res. 146, 41–50.

Kato, N., Nakamura, T., Dansako, H., Namba, K., Abe, K., Nozaki, A., Naka, K., Ikeda, M., Shimotohno, K., 2005. Genetic variation and dynamics of hepatitis C virus replicons in long-term cell culture. J. Gen. Virol. 86, 645–656.

Kato, N., Sugiyama, K., Namba, K., Dansako, H., Nakamura, T., Takami, M., Naka, K., Nozaki, A., Shimotohno, K., 2003. Establishment of a hepatitis C virus subgenomic replicon derived from human hepatocytes infected in vitro. Biochem. Biophys. Res. Commun. 306, 756–766.

Lau, J.Y., Tam, R.C., Liang, T.J., Hong, Z., 2002. Mechanism of action of ribavirin in the combination treatment of chronic HCV infection. Hepatology 35, 1002–1009.

Liu, W.L., Su, W.C., Cheng, C.W., Hwang, L.H., Wang, C.C., Chen, H.L., Chen, D.S., Lai, M.Y., 2007. Ribavirin up-regulates the activity of double-stranded RNA-activated protein kinase and enhances the action of interferon-alpha against hepatitis C virus. J. Infect. Dis. 196, 425–434.

Lohmann, V., Overton, H., Bartenschlager, R., 1999. Selective stimulation of hepatitis C virus and pestivirus NS5B RNA polymerase activity by GTP. J. Biol. Chem. 274, 10807–10815.

Luo, G., Hamatake, R.K., Mathis, D.M., Racela, J., Rigat, K.L., Lemm, J., Colonno, R.J., 2000. De novo initiation of RNA synthesis by the RNA-dependent RNA polymerase (NS5B) of hepatitis C virus. J. Virol. 74, 851–863.

Marcellin, P., Horsmans, Y., Nevens, F., Grange, J.D., Bronowicki, J.P., Vetter, D., Purdy, S., Garg, V., Bengtsson, L., McNair, L., Alam, J., 2007. Phase 2 study of the combination of merimepodib with peginterferon-alpha2b, and ribavirin in nonresponders to previous therapy for chronic hepatitis C. J. Hepatol. 47, 476–483.

McHutchison, J.G., Shiffman, M.L., Cheung, R.C., Gordon, S.C., Wright Jr., T.L., Pottage, J.C., McNair, L., Ette, E., Moseley, S., Alam, J., 2005. A randomized, double-blind, placebo-controlled dose-escalation trial of merimepodib (VX-497) and interferon-alpha in previously untreated patients with chronic hepatitis C. Antivir. Ther. 10, 635–643.

Mori, K., Ikeda, M., Ariumi, Y., Kato, N., 2010. Gene expression profile of Li23, a new human hepatoma cell line that enables robust hepatitis C virus replication, Comparison with HuH-7 and other hepatic cell lines. Hepatol. Res. 40, 1248–1253.

Naka, K., Ikeda, M., Abe, K., Dansako, H., Kato, N., 2005. Mizoribine inhibits hepatitis C virus RNA replication, effect of combination with interferon-alpha. Biochem. Biophys. Res. Commun. 330, 871–879.

Pastor-Anglada, M., Cano-Soldado, P., Molina-Arcas, M., Lostao, M.P., Larráyoz, I., Martínez-Picado, J., Casado, F.J., 2005. Cell entry and export of nucleoside analogues. Virus Res. 107, 151–164.

Pawlotsky, J.M., Dahari, H., Neumann, A.U., Hezode, C., Germanidis, G., Lonjon, I., Castera, L., Dhumeaux, D., 2004. Antiviral action of ribavirin in chronic hepatitis C. Gastroenterology 126, 703–714.

Rustgi, V.K., Lee, W.M., Lawitz, E., Gordon, S.C., Afdhal, N., Poordad, F., Bonkovsky, H.L., Bengtsson, L., Chandorkar, G., Harding, M., McNair, L., Aalyson, M., Alam, J., Kauffman, R., Gharakhanian, S., McHutchison, J.G., MErimepodib TRiple cOmbination Study Group, 2009. Merimepodib, pegylated interferon, and ribavirin in genotype 1 chronic hepatitis C pegylated interferon and ribavirin nonresponders. Hepatology 50, 1719–1726.

Simister, P., Schmitt, M., Geitmann, M., Wicht, O., Danielson, U.H., Klein, R., Bressanelli, S., Lohmann, V., 2009. Structural and functional analysis of hepatitis C virus strain JFH1 polymerase. J. Virol. 83, 11926–11939.

Tanabe, Y., Sakamoto, N., Enomoto, N., Kurosaki, M., Ueda, E., Maekawa, S., Yamashiro, T., Nakagawa, M., Chen, C.H., Kanazawa, N., Kakinuma, S., Watanabe, M., 2004. Synergistic inhibition of intracellular hepatitis C virus replication by combination of ribavirin and interferon-alpha. J. Infect. Dis. 189, 1129–1139.

Thomas, D.L., 2000. Hepatitis C epidemiology. Curr. Top. Microbial. Immunol. 242, 25–41.

Thomas, E., Feld, J.J., Li, Q., Hu, Z., Fried, M.W., Liang, T.J., 2011. Ribavirin potentiates interferon action by augmenting interferon-stimulated gene induction in HCV cell culture models. Hepatology 53, 32–41.

Wakita, T., Pietschmann, T., Kato, T., Date, T., Miyamoto, M., Zhao, Z., Murthy, K., Habermann, A., Kräusslich, H.G., Mizokami, M., Bartenschlager, R., Liang, T.J., 2005. Production of infectious hepatitis C virus in tissue culture from a cloned viral genome. Nat. Med. 11, 791–796.

Wang, J., Yang, J.W., Zeevi, A., Webber, S.A., Girnita, D.M., Selby, R., Fu, J., Shah, T., Pravica, V., Hutchinson, I.V., Burckart, G.J., 2008. IMPDH1 gene polymorphisms and association with acute rejection in renal transplant patients. Clin. Pharmacol. Ther. 83, 711–717.

Yano, M., Ikeda, M., Abe, K., Dansako, H., Ohkoshi, S., Aoyagi, Y., Kato, N., 2007. Comprehensive analysis of the effects of ordinary nutrients on hepatitis C virus RNA replication in cell culture. Antimicrob. Agents Chemother. 51, 2016–2127.

Yano, M., Ikeda, M., Abe, K., Kawai, Y., Kuroki, M., Mori, K., Dansako, H., Ariumi, Y., Ohkoshi, S., Aoyagi, Y., Kato, N., 2009. Oxidative stress induces anti-hepatitis C virus status via the activation of extracellular signal-regulated kinase. Hepatology 50, 678–688.

Zhou, S., Liu, R., Baroudy, B.M., Malcolm, B.A., Reyes, G.R., 2003. The effect of ribavirin and IMPDH inhibitors on hepatitis C virus subgenomic replicon RNA. Virology 310, 333–342.

Liver INTERNATIONAL
OFFICIAL JOURNAL OF THE INTERNATIONAL ASSOCIATION FOR THE STUDY OF THE LIVER

Liver International ISSN 1478-3223

BASIC STUDIES

Anti-ulcer agent teprenone inhibits hepatitis C virus replication: potential treatment for hepatitis C

Masanori Ikeda[1]*, Yoshinari Kawai[1,2]*, Kyoko Mori[1], Masahiko Yano[1,3], Ken-ichi Abe[1], Go Nishimura[1], Hiromichi Dansako[1], Yasuo Ariumi[1], Takaji Wakita[4], Kazuhide Yamamoto[2] and Nobuyuki Kato[1]

1 Department of Tumor Virology, Okayama University Graduate School of Medicine, Dentistry, and Pharmaceutical Sciences, Okayama, Japan
2 Department of Gastroenterology and Hepatology, Okayama University Graduate School of Medicine, Dentistry, and Pharmaceutical Sciences, Okayama, Japan
3 Division of Gastroenterology and Hepatology, Graduate School of Medical and Dental Sciences, Niigata University, Niigata City, Japan
4 Department of Virology II, National Institute of Infectious Diseases, Tokyo, Japan

Keywords
geranylgeranylation – HCV – Selbex – statin – teprenone

Correspondence
Masanori Ikeda, MD, PhD, Department of Tumor Virology, Okayama University Graduate School of Medicine, Dentistry, and Pharmaceutical Sciences, 2-5-1 Shikata-cho, Okayama 700-8558, Japan
Tel: +81-86-235-7386
Fax: +81-86-235-7392
e-mail: maikeda@md.okayama-u.ac.jp

Received 11 October 2010
Accepted 7 February 2011

DOI:10.1111/j.1478-3231.2011.02499.x

Abstract

Background: Previously we reported that 3-hydroxy-3-methylglutaryl coenzyme A reductase inhibitors, statins, inhibited hepatitis C virus (HCV) RNA replication. Furthermore, recent reports revealed that the statins are associated with a reduced risk of hepatocellular carcinoma and lower portal pressure in patients with cirrhosis. The statins exhibited anti-HCV activity by inhibiting geranylgeranylation of host proteins essential for HCV RNA replication. Geranylgeranyl pyrophosphate (GGPP) is a substrate for geranylgeranyltransferase. Therefore, we examined the potential of geranyl compounds with chemical structures similar to those of GGPP to inhibit HCV RNA replication. *Methods:* We tested geranyl compounds [geranylgeraniol, geranylgeranoic acid, vitamin K_2 and teprenone (Selbex)] for their effects on HCV RNA replication using genome-length HCV RNA-replicating cells (the OR6 assay system) and a JFH-1 infection cell culture system. Teprenone is the major component of the anti-ulcer agent, Selbex. We also examined the anti-HCV activities of the geranyl compounds in combination with interferon (IFN)-α or statins. *Results:* Among the geranyl compounds tested, only teprenone exhibited anti-HCV activity at a clinically achievable concentration. However, other anti-ulcer agents tested had no inhibitory effect on HCV RNA replication. The combination of teprenone and IFN-α exhibited a strong inhibitory effect on HCV RNA replication. Although teprenone alone did not inhibit geranylgeranylation, surprisingly, statins' inhibitory action against geranylgeranylation was enhanced by cotreatment with teprenone. *Conclusions:* The anti-ulcer agent teprenone inhibited HCV RNA replication and enhanced statins' inhibitory action against geranylgeranylation. This newly discovered function of teprenone may improve the treatment of HCV-associated liver diseases as an adjuvant to statins.

Hepatitis C virus (HCV) infection frequently causes persistent hepatitis and leads to cirrhosis and hepatocellular carcinoma (HCC). Currently, the combination therapy of pegylated interferon (IFN) with ribavirin is available for patients with chronic hepatitis C (CH C) and yields a sustained virological response rate of about 50% (1). However, about half of CH C patients are still susceptible to the progression of the disease to fatal cirrhosis and HCC. Therefore, the development of more effective reagents for the treatment of HCV infection is urgent.

To overcome this problem, we developed a genome-length HCV RNA (strain O of genotype 1b) replication system (OR6) with luciferase as a reporter, which facilitated the prompt and precise monitoring of HCV RNA replication in hepatoma cells (HuH-7-derived OR6 cells) (2). Using this OR6 system, we recently reported that 3-hydroxy-3-methylglutaryl coenzyme A (HMG-CoA) reductase inhibitors, statins, inhibited HCV RNA replication efficiently (3–5). Among five statins – fluvastatin (FLV), atorvastatin (ATV), simvastatin (SIV), pravastatin (PRV) and lovastatin (LOV) – FLV exhibited the strongest anti-HCV activity, while PRV had no effect on HCV RNA replication (3, 6). More recently, Bader *et al.* (7) demonstrated that FLV inhibited HCV RNA replication

*Contributed equally.

in humans. Furthermore, recent reports revealed that the statins were associated with a reduced risk of HCC (8) and lower portal pressure in patients with cirrhosis (9).

Statins targeted the mevalonate pathway. This pathway is branched after farnesyl pyrophosphate (FPP) into cholesterol and geranylgeranyl pyrophosphate (GGPP) biosynthesis pathways. The inhibition of GGPP but not of cholesterol is essential for HCV RNA replication in the inhibitory activity of statins (3, 10, 11). To date, one of the proteins, FBL2, was reported as the host protein essential for HCV RNA replication. HCV RNA replication requires geranylgeranylation of FBL2 by geranylgeranyltransferase with GGPP (12).

We have attempted to examine the effects of geranyl compounds [geranylgeraniol (GGOH), geranylgeranoic acid, vitamin K_2 (VK2) and teprenone] on HCV RNA replication using the OR6 assay system and the JFH-1 infection cell culture system, because their chemical formulas are similar to that of the GGPP, a substrate for geranylgeranyltransferase in geranylgeranylation (13–15). The anti-ulcer agent teprenone (also called geranylgeranylacetone) is reported to block the function of GGPP by the competitive inhibition of the mevalonate pathway (16). Teprenone is the major component of the clinically used anti-ulcer reagent, Selbex.

Here, we reported the inhibitory activity of teprenone on HCV RNA replication and the effect of teprenone in combination with statins on their inhibitory action against geranylgeranylation.

Materials and methods

Reagents and antibodies

Teprenone (Selbex), geranylgeranoic acid, ecabet sodium and sofalcon, gefarnate were purchased from Eisai Co. Ltd (Tokyo, Japan), BIOMOL (Plymouth Meeting, PA, USA), Mitsubishi Tanabe Pharma (Osaka, Japan), Taisho Pharmaceutical Co. (Tokyo, Japan) and Dainippon Sumitomo Pharma Co. Ltd (Osaka, Japan) respectively. GGPP, GGOH, VK2, IFN-α, vitamin E, linoleic acid and mevalonate were purchased from Sigma (St Louis, MO, USA). Cyclosporine A, FLV, LOV and PRV were purchased from Calbiochem (Los Angeles, CA, USA). ATV, SIV and pitavastatin (PTV) were purchased from Astellas Pharma Inc. (Tokyo, Japan), Banyu Pharmaceutical Co. Ltd (Tokyo, Japan), and Kowa Co. Ltd (Nagoya, Japan) respectively.

The antibodies used in this study were those specific to the Core (CP11, Institute of Immunology, Tokyo), NS5A (a generous gift from Dr A. Takamizawa, Research Foundation for Microbial Diseases, Osaka University), NS5B (a generous gift from Dr M. Kohara, Tokyo Metropolitan Institute of Medical Science) and β-actin (Sigma). Anti-heat shock protein (HSP) 90 and anti-HSP70 antibodies were purchased from BD Bioscience (San Jose, CA, USA). Anti-Rap1A (sc-1482) and anti-Rap1 (sc-65) antibodies were purchased from Santa Cruz Biotechnology (Santa Cruz, CA, USA).

Cell cultures

OR6 is a cell line cloned from ORN/C-5B/KE RNA-replicating HuH-7 cells as described previously (2) and cultured in Dulbecco's modified Eagle's medium supplemented with 10% fetal bovine serum, penicillin, streptomycin and G418 (300 μg/ml; Geneticin, Invitrogen, Carlsbad, CA, USA). ORN/C-5B/KE RNA is derived from HCV-O, and OR6c cells are cured OR6 cells from which HCV RNA was eliminated by IFN-α treatment as described previously (2). HCV-O/RLGE is the authentic HCV RNA containing adaptive mutations of Q1112R, P1115L, E1203G and K1609E in the NS3 region and replicates efficiently in OR6c cells.

OR6 reporter assay

For the *Renilla* luciferase (RL) assay, $1.0–1.5 \times 10^4$ OR6 cells were plated onto 24-well plates in triplicate and precultured for 24 h. The cells were treated with each compound for 72 h. Then, the cells were harvested and subjected to an RL assay according to the manufacturer's protocol (2).

Western blot analysis

For western blot analysis, $4–4.5 \times 10^4$ OR6 or OR6c cells harbouring HCV-O/RLGE RNA were plated onto six-well plates and cultured for 24 h, and were then treated with each compound for 72 h. Preparation of the cell lysates, sodium dodecyl sulphate-polyacrylamide gel electrophoresis and immunoblotting were then performed as described previously (17).

Cell growth assay

To examine the effect of each reagent on OR6 cell growth, $6.0–6.5 \times 10^4$ OR6 cells were plated onto six-well plates in triplicate and were precultured for 24 h. The cells were treated with or without each compound for 72 h, and then the viable cells were counted after trypan blue dye treatment as described previously (18).

WST-1 cell proliferation assay

The OR6 cells (2×10^3 cells) were plated onto a 96-well plate in triplicate at 24 h before treatment with each reagent. The cells at 24, 48 and 72 h after treatment were subjected to a WST-1 cell proliferation assay (Takara Bio, Otsu, Japan) according to the manufacturer's protocol.

Reverse transcription-polymerase chain reaction

Reverse transcription-polymerase chain reaction (RT-PCR) for HMG-CoA reductase and for glyceraldehyde-3-phosphate dehydrogenase (GAPDH) was performed by a method described previously (19). Briefly, using cellular total RNAs (2 μg), cDNA was synthesized using Superscript II with the oligo dT primer. One-tenth of the synthesized cDNA was subjected to PCR with the

following primer pairs: HMG-CoA reductase, 5′-ATGCC ATCCCTGTTGGAGTG-3′ and 5′-TGTTCATCCCCATG GCATCCC-3′; and GAPDH, 5′-GACTCATGACCACAG TCCATGC-3′ and 5′-GAGGAGACCACCTGGTGCTCA G-3′.

Hepatitis C virus infection experiment

For the infection experiment with the JFH-1 virus, HuH-7-derived RSc cells (1×10^5 cells) were plated onto six-well plates and cultured for 24 h (20). Then, the cells were infected with 100 µl (equivalent to a multiple of infection of 0.1–0.2) of inoculum and cultured for 24 h. The cells were treated with each reagent for 72 h. The culture supernatants and cells were collected for quantification of the Core by an enzyme-linked immunosorbent assay (ELISA) (Mitsubishi Kagaku Bio-Clinical Laboratories, Tokyo, Japan) and for western blot analysis respectively.

Statistical analysis

The luciferase activities were statistically compared between the various treatment groups using Student's *t*-test. *P* values of < 0.05 were considered statistically significant. The mean ± standard deviation is determined from at least three independent experiments.

Results

Anti-hepatitis C virus activity of teprenone is a unique feature not only among geranyl compounds but also among anti-ulcer agents

The mevalonate pathway is divided into two branches: cholesterol synthesis and GGPP synthesis pathways (Fig. 1). The statins exhibited anti-HCV activity via inhibition of geranylgeranylation of host proteins essential for HCV RNA replication. Therefore, we examined the effects of geranyl compounds [GGOH, geranylgeranoic acid, VK2 and teprenone (Selbex)] on HCV RNA replication using the OR6 assay system, because their chemical structures are similar to that of the GGPP (Fig. 2A) (16). Teprenone inhibited HCV RNA replication in a dose-dependent manner without affecting OR6 cell growth up to a concentration of 20 µg/ml (Fig. 2B). The 50% effective concentration (EC_{50}) of teprenone is 5.3 µg/ml. On the other hand, GGOH, geranylgeranoic acid and VK2 did not inhibit HCV RNA replication at the concentration without cytotoxicity (Fig. 2C–E). We also demonstrated that teprenone did not affect cell proliferation within this concentration (supporting information, Fig. S1A). These results suggest that anti-HCV activity of teprenone was not a common feature among geranyl compounds.

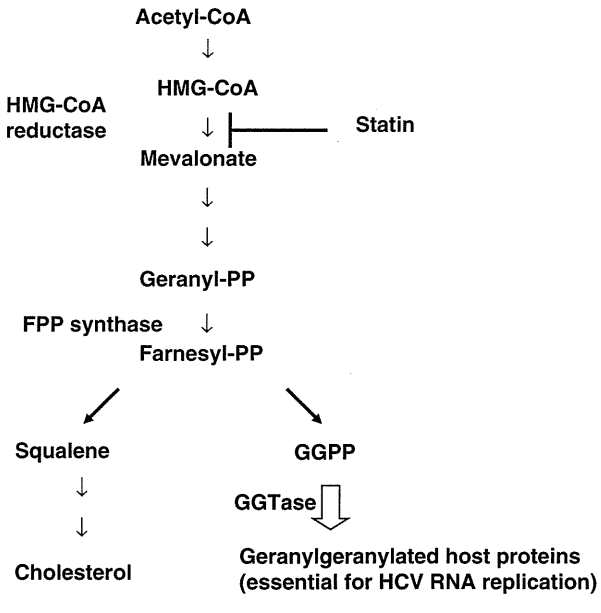

Fig. 1. Schema of the mevalonate pathway.

Teprenone is used for patients with gastritis and gastric ulcers. Therefore, we examined anti-ulcer agents for their inhibitory effects against HCV RNA replication. The chemical structures of three anti-ulcer agents – ecabet sodium, sofalcon and gefarnate – are shown in supporting information, Figure S1B. None of these agents exhibited inhibitory effects on HCV RNA replication (supporting information, Fig. S1C–E). These results indicate that the anti-HCV activity of teprenone may not be a common feature among anti-ulcer agents.

Teprenone inhibited authentic hepatitis C virus RNA replication

The genome-length HCV RNA replicating in the OR6 cells contained three non-natural elements – RL, neomycin phosphotransferase and encephalomyocarditis virus internal ribosomal entry site. To further confirm that the anti-HCV activity of teprenone was not because of the inhibition of these three exogenous genes or their products, we used authentic 9.6 kb HCV RNA-replicating cells. We introduced *in vitro* synthesized HCV-O/RLGE RNA into cured OR6c cells (Fig. 3A). As shown in Figure 3B, teprenone inhibited Core expression in HCV-O/RLGE-replicating OR6c cells in a dose-dependent manner. These results indicate that the anti-HCV activity of teprenone was because of the inhibition of HCV RNA itself, but not exogenous genes or their products.

Teprenone enhanced anti-hepatitis C virus activity of interferon-α

We examined whether or not teprenone would enhance the anti-HCV activity of IFN-α. We did this by studying the inhibitory effects of combinations of IFN-α (0, 2.5, 5 and 10 IU/ml) and teprenone (0, 10 and 20 µg/ml) using the OR6 assay system. Teprenone enhanced the anti-HCV activity of IFN-α in a dose-dependent manner (Fig. 4). Teprenone with IFN-α also inhibited Core expression (Fig. 4). We also demonstrated that teprenone did not

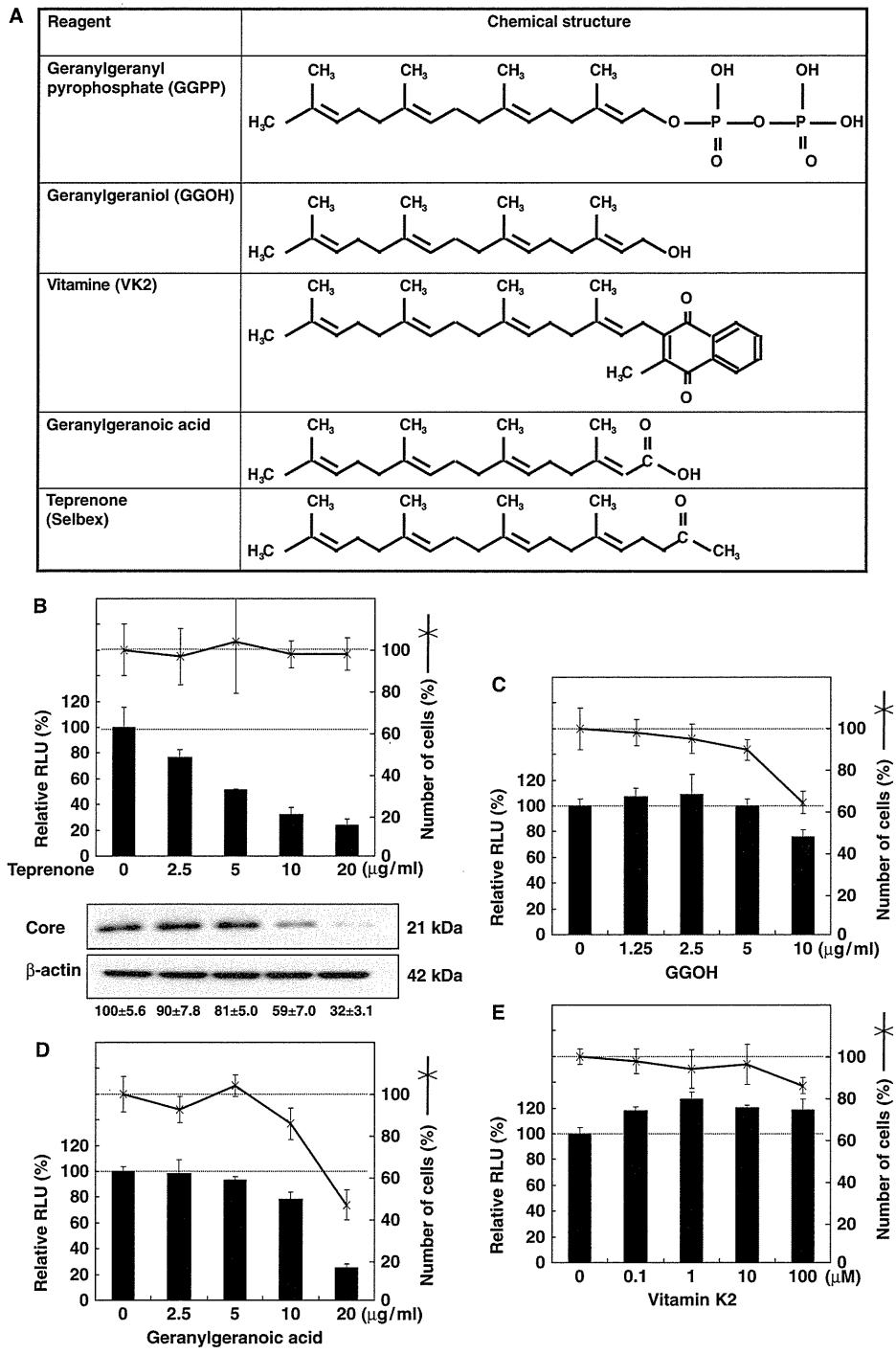

Fig. 2. The effects of geranyl compounds and anti-ulcer agents on hepatitis C virus (HCV) RNA replication. (A) Structures of geranyl compounds. (B) Anti-HCV activity of teprenone on HCV RNA replication in OR6 cells. OR6 cells were treated with teprenone (0, 2.5, 5, 10 and 20 μg/ml) for 72 h. *Renilla* luciferase (RL) activity for HCV RNA replication is shown as a percentage of control. Each bar represents the average with standard deviations of triplicate data points. Cell viability was also shown as a percentage of control. After 72-h treatment, the production of the Core was analysed by immunoblotting using anti-Core antibody (lower panel). β-actin was used as a control for the amount of protein loaded per lane. The signal intensities of Core from three independent assays were quantified by densitometry and normalized by that of β-actin. Each of the mean ± standard deviation is under the lower panel. (C to E) OR6 cells were treated with geranylgeraniol (0, 1.25, 2.5, 5 and 10 μg/ml) (C), geranylgeranoic acid (0, 2.5, 5, 10 and 20 μg/ml) (D) and VK2 (0, 0.1, 1, 10 and 100 μM) (E) for 72 h. RL activity and cell viability after treatment were determined as shown in (B).

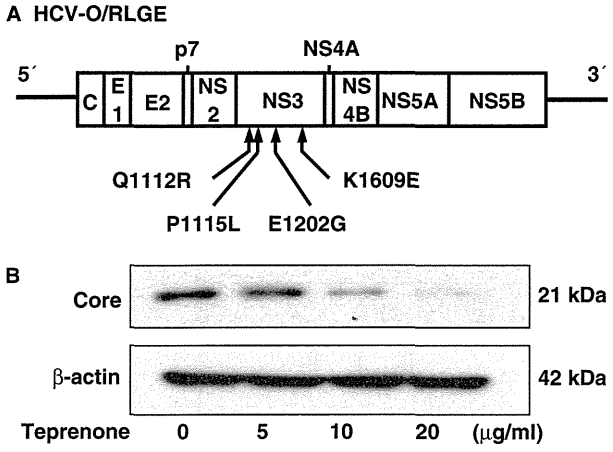

Fig. 3. Teprenone inhibited authentic hepatitis C virus (HCV) RNA replication. (A) Schematic gene organization of genome-length HCV-O/RLGE RNA. The positions of four adaptive mutations – Q1112R, P1115L, E1203G and K1609E – are indicated by arrows. (B) HCV-O/RLGE RNA was introduced into OR6c cells by electroporation as described previously (5). The cells were treated with teprenone (0, 5, 10 and 20 μg/ml) for 72 h and then the production of the Core was analysed by immunoblotting using anti-Core antibody.

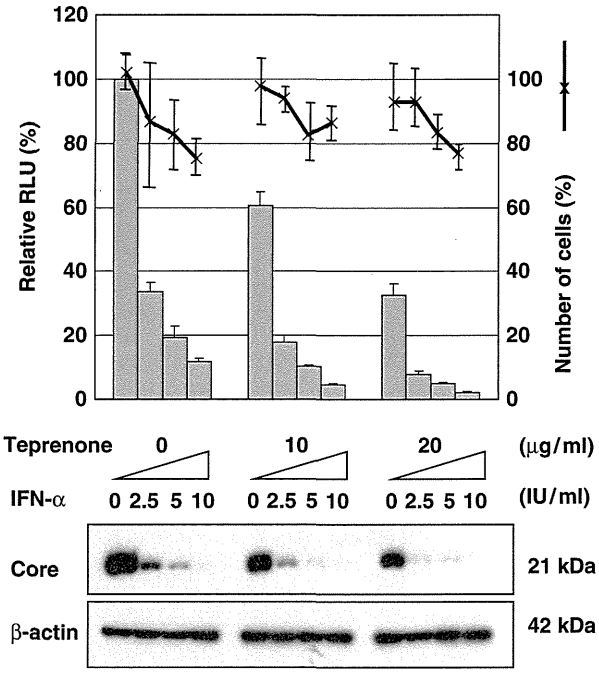

Fig. 4. Teprenone enhanced the anti-hepatitis C virus activity of interferon (IFN)-α. OR6 cells were cotreated with IFN-α (0, 2.5, 5 and 10 IU/ml) and teprenone (0, 10 and 20 μg/ml) for 72 h. *Renilla* luciferase assay was performed as described in Figure 2B. Production of the Core was analysed by immunoblotting using anti-Core antibody. The cells at 24, 48 and 72 h after treatment were subjected to a WST-1 cell proliferation assay.

affect cell proliferation within this concentration (Fig. 4). These results suggest that teprenone may be a new candidate as a complement to IFN therapy.

Teprenone exhibited anti-hepatitis C virus activity in the JFH-1 infection system

We examined the anti-HCV activity of teprenone in the JFH-1 infection system (13–15). We treated the cells with teprenone (0, 5, 10 and 20 μg/ml) at 24-h post-JFH-1 infection and cultured them for 72 h. The culture supernatants and cells were subjected to quantification of the Core by ELISA and western blot analysis respectively. Teprenone decreased the HCV Core in the supernatant (upper panel in Fig. 5A) and in the cells (lower panel in Fig. 5A) in a dose-dependent manner.

We next tested whether or not teprenone (0, 10 and 20 μg/ml) enhanced IFN-α's (0, 2.5 and 5 IU/ml) anti-HCV activity in the JFH-1 infection system. As shown in Figure 5B, teprenone enhanced the anti-HCV activity of IFN-α in a dose-dependent manner. These results suggest that teprenone also possessed anti-HCV activity in the JFH-1 infection system.

Teprenone did not inhibit geranylgeranylation

As shown in Figure 2A, the chemical structure of teprenone is similar to that of GGPP. Therefore, we examined the possibility that teprenone inhibits geranylgeranylation. Geranylgeranyl proteins possessed the C-A-A-X motif at the C-terminal of the protein: C is cystein; A is aliphatic amino acid; and X is typically leucine (or rarely isoleucine, valine or phenylalanine). Rap1A is one of the Ras-related proteins and selected to monitor the status of geranylgeranylation. We used anti-Rap1A antibody (sc-1482), which recognized only nongeranylgeranylated Rap1A (21, 22). Therefore, geranylgeranylated Rap1A is not recognized with this antibody. On the other hand, anti-Rap1 antibody (sc-65) recognizes Rap1A and Rap1B independent of the state of geranylgeranylation (22). In the following experiments, we used anti-Rap1A antibody (sc-1482) to monitor the state of geranylgeranylation.

OR6 cells were treated with PTV (1.25 μM) or teprenone (20 μg/ml) or neither. The cells were collected after treatment and subjected to luciferase assay and western blot analysis. In the untreated cells, nongeranylgeranylated Rap1A bands were not detected (Fig. 6A). PTV inhibited geranylgeranylation at 3 h and reached a plateau 12 h after treatment along with nongeranylgeranylated Rap1A bands (Fig. 6A). On the other hand, geranylgeranylation was not inhibited in the cells with teprenone treatment (Fig. 6A).

We then tested the effect of mevalonate cotreatment with PTV or teprenone. Mevalonate negated PTV's inhibitory action against geranylgeranylation and led to the loss of PTV's anti-HCV activity (Fig. 6B). However, mevalonate did not affect the anti-HCV activity of teprenone (Fig. 6B). These results indicate that teprenone

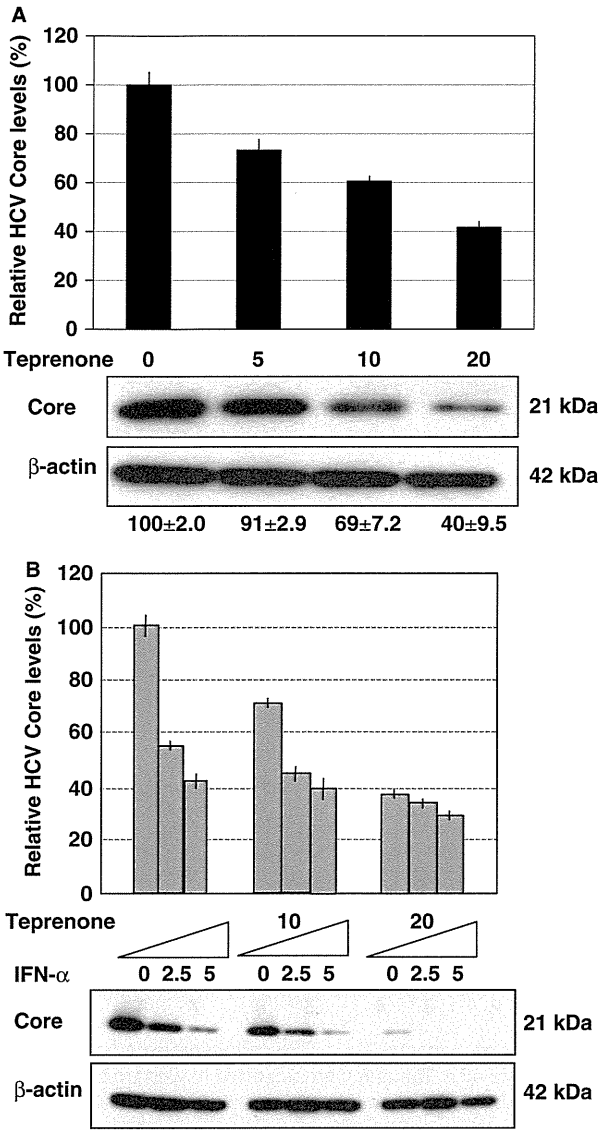

Fig. 5. Teprenone exhibited anti-hepatitis C virus (HCV) activity in the JFH-1 infection system. (A) Teprenone inhibited JFH-1 replication. HuH-7-derived RSc cells were infected with the JFH-1 virus for 24 h and were then treated with teprenone (0, 5, 10 and 20 μg/ml) for 72 h. The supernatant and the cells were subjected to quantification of the Core by ELISA and western blot analysis respectively. The signal intensities of Core were quantified by densitometry and the mean ± standard deviation is under the lower panel as shown in Figure 2B. (B) Teprenone enhanced interferon (IFN)-α's anti-HCV activity in the JFH-1 infection system. JFH-1 virus-infected cells were treated with teprenone (0, 10 and 20 μg/ml) and IFN-α (0, 2.5 and 5 IU/ml) for 72 h and then subjected to Core quantification by ELISA and western blot analysis as shown in (A).

inhibits HCV RNA replication without the inhibition of geranylgeranylation.

Statin's inhibition of HMG-CoA reductase decreased cholesterol synthesis and led to the increase of HMG-CoA reductase expression by positive feedback (3). The mRNA of HMG-CoA reductase was increased with PTV treatment but not with teprenone treatment (supporting information, Fig. S3A and B). This result suggests that teprenone, unlike PTV, did not lower the cholesterol synthesis.

The chemical structure of teprenone, which is the major component of Selbex, is similar to that of GGPP, a substrate for geranylgeranyltransferase. Therefore, we ruled out the possibility that teprenone was incorporated into host proteins instead of GGPP and led to the loss of function of the host proteins, when endogenous GGPP was depleted by PTV in OR6 cells. The nongeranylgeranylated Rap1A was detected when OR6 cells were treated with PTV (lane 3; Fig. 6C). However, exogenous GGPP decreased nongeranylgeranylated Rap1A in PTV-treated OR6 cells (lane 4; Fig. 6C). If teprenone was incorporated into Rap1A instead of GGPP and formed a psuedo-geranylgeranylation, Rap1A blotted with anti-Rap1A (sc-1482) would be decreased. Surprisingly, non-geranylgeranylated Rap1A increased in OR6 cells after treatment with PTV and teprenone (compare lanes 3 and 7 in Fig. 6C). Furthermore, it is noteworthy that the total amount of Rap1 was decreased when OR6 cells were treated with PTV and teprenone. These results suggest that teprenone was not incorporated into host protein and unexpectedly enhanced the statin's inhibitory action against geranylgeranylation.

Teprenone enhanced statins' inhibitory action against geranylgeranylation

To further investigate the unexpected results shown in Figure 6C, we tested the geranylgeranyl state and anti-HCV activity using the OR6 assay system. OR6 cells were treated with teprenone (0, 10 and 20 μg/ml) in combination with PTV (0, 0.25, 0.5 and 1.0 μM) for 72 h and subjected to western blot analysis for the geranylgeranyl state using anti-Rap1A (sc-1482) and anti-Rap1 (sc-65) antibodies, and for anti-HCV activity using anti-Core, anti-NS5A and anti-NS5B antibodies. Anti-HCV activity was also assessed by a luciferase reporter assay. Teprenone by itself did not inhibit geranylgeranylation (lanes 1–3; Fig. 7A). When teprenone was treated with PTV (0.25 μM), nongeranylgeranylated Rap1A increased in a dose-dependent manner (lanes 4–6; Fig. 7A). This result indicates that teprenone enhanced PTV's inhibitory action against geranylgeranylation in a dose-dependent manner. This effect of teprenone was also confirmed when PTV was treated at concentrations of 0.5 and 1.0 μM (lanes 7–12; Fig. 7A). HCV RNA replication and the expression of HCV proteins were decreased when nongeranylgeranylated Rap1As were increased. Next, we examined whether or not this function of teprenone is a common feature against statins. Teprenone enhanced the inhibitory action of ATV, SIV, FLV and LOV but not PRV against geranylgeranylation (lower panel in Fig. 7B). Teprenone also enhanced anti-HCV activity in combination with statins (upper panel in Fig. 7B). These results

Liver International (2011)

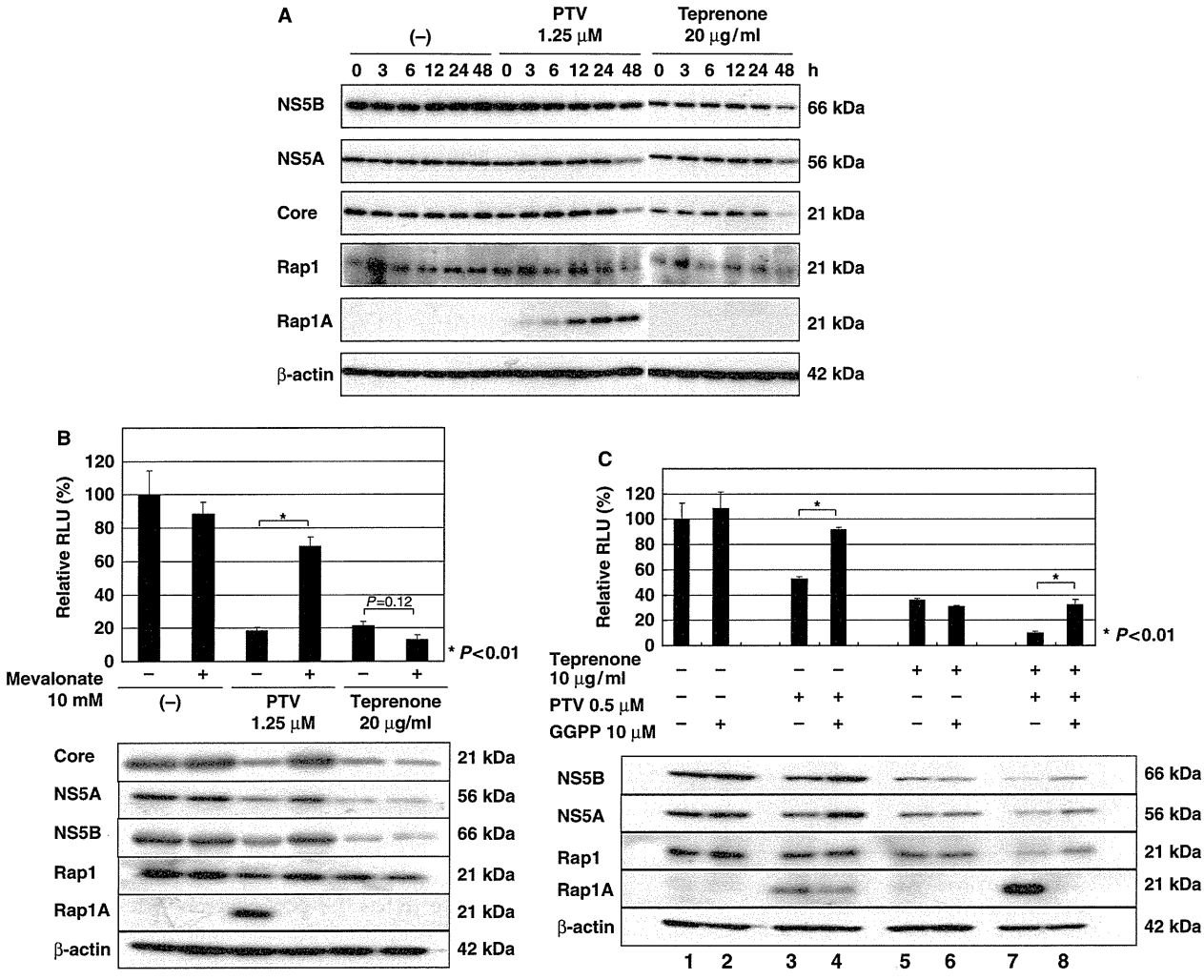

Fig. 6. Teprenone did not inhibit geranylgeranylation. (A) Teprenone did not inhibit geranylgeranylation. OR6 cells were treated with pitavastatin (PTV) (1.25 μM) or teprenone (20 μg/ml), or neither for 0, 3, 6, 12, 24 and 48 h. The cells were subjected to western blot analysis for HCV proteins using anti-NS5B, anti-NS5A and anti-Core antibodies, and for geranylgeranylation assay using anti-Rap1A (sc-1482) and anti-Rap1 (sc-65) antibodies. (B) Mevalonate did not affect the anti-HCV activity of teprenone. OR6 cells were treated with PTV (1.25 μM), teprenone (20 μg/ml) or neither in the absence or in the presence of mevalonate (10 mM) for 72 h. Then the cells were subjected to luciferase assay (upper panel) and western blot analysis using anti-Core, anti-NS5A, anti-NS5B, anti-Rap1A (sc-1482), anti-Rap1 (sc-65) and anti-β-actin antibodies (lower panel), as shown in (A). (C) Teprenone was not used as a substrate for GGT after the depletion of geranylgeranyl pyrophosphate (GGPP) by statin. OR6 cells were treated with teprenone (0 and 10 μg/ml), PTV (0 and 0.5 μM) and GGPP (0 and 10 μM) in the indicated combination for 72 h. Then the cells were subjected to luciferase assay (upper panel) and geranylgeranyl assay using anti-Rap1A (sc-1482) and anti-Rap1 (sc-65) antibodies (lower panel) as shown in (A).

suggest that teprenone enhances statins' inhibitory action against geranylgeranylation, except for PRV.

Discussion

In this study, we demonstrated that teprenone inhibited HCV RNA replication. Furthermore, teprenone exhibited anti-HCV activity in the genotype-2a JFH-1 infection system. Teprenone belongs to the geranyl compounds from its chemical structure and anti-ulcer agent from its clinical application. Therefore, we tested other geranyl compounds (GGOH and VK2, as well as geranylgeranoic acid) and other anti-ulcer agents (ecabet sodium, sofalcone and gefarnate) for their effect on HCV RNA replication. However, only teprenone exhibited anti-HCV activity among the reagents tested. Therefore, the anti-HCV activity of teprenone is a unique feature among these reagents.

The interview form from Selbex providing company Eisai reported the plasma concentration of teprenone. When 150 mg of Selbex was administered orally, its maximum plasma concentration reached 2.2 μg/ml. This is similar to the EC_{50} (5.3 μg/ml) of Selbex *in vitro*.

Ichikawa *et al.* (23) reported that teprenone induced the 2′,5′-oligoadenylate synthetases (2′5′-OAS) in

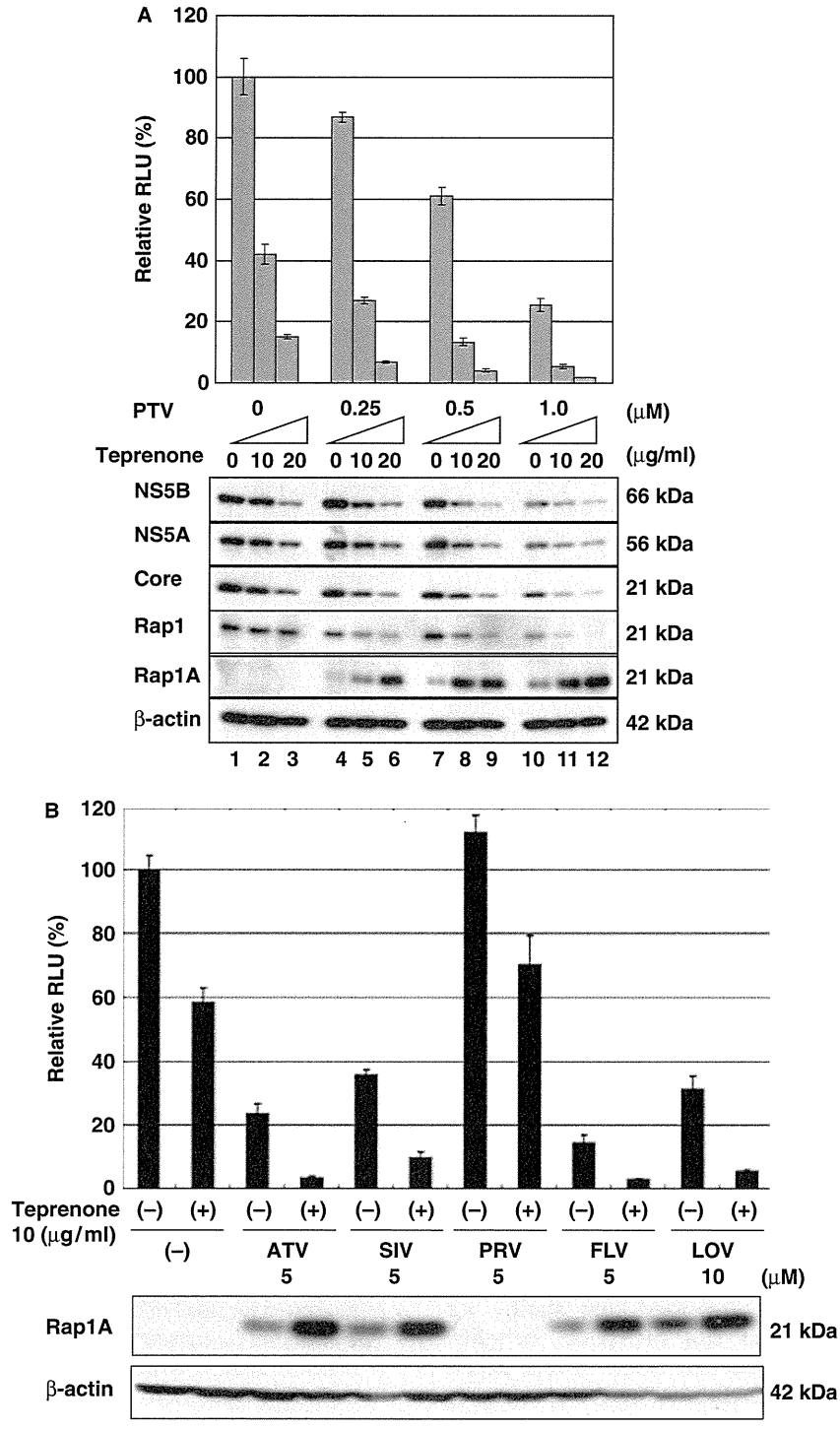

Fig. 7. Teprenone enhanced statins' inhibitory action against geranylgeranylation. (A) Teprenone enhanced pitavastatin (PTV)'s inhibitory action against geranylgeranylation. OR6 cells were treated with teprenone (0, 10 and 20 μg/ml) and PTV (0, 0.25, 0.5 and 1.0 μM) for 72 h. Then the cells were subjected to luciferase assay (upper panel) and western blot analysis using anti-NS5A, anti-Rap1A (sc-1482) and anti-Rap1 (sc-65), and anti-β-actin antibodies (lower panel), as shown in Figure 6A. (B) Teprenone enhanced statins' [except for pravastatin (PRV)] inhibitory action against geranylgeranylation. OR6 cells were treated with teprenone (0, 10 μg/ml) and atorvastatin (0, 5 μM), simvastatin (0, 5 μM), PRV (0, 5 μM), fluvastatin (0, 5 μM) and lovastatin (0, 10 μM) for 72 h. Then the cells were subjected to luciferase assay (upper panel) and western blot analysis using anti-Rap1A (sc-1482), and anti-β-actin antibodies (lower panel), as shown in Figure 6A.

Liver International (2011)

human hepatoma cells. We demonstrated the activation of 2′5′-OAS and IFN-stimulated response element (ISRE) by IFN-α using the reporter assay system in our HuH-7-derived OR6 cells. However, we could not obtain evidence that teprenone activated both 2′5′-OAS and ISRE promoters (supporting information, Fig. S2A and B). Signal transducer and activator of transcription (STAT)1 and STAT2 were not phosphorylated after treatment with teprenone (supporting information, Fig. S2C). This discrepancy may have been caused by the heterogeneity of HuH-7 cells, because OR6 was selected as the clonal cell line and is highly susceptible to HCV RNA replication. Further study is needed to clarify the mechanism underlying teprenone's effect on IFN signalling.

Teprenone reportedly protects the gastric mucosa by inducing HSP (24). From this standpoint, the anti-HCV activity of teprenone was an unexpected result, because recently, it was reported that HSP90 is essential for HCV RNA replication and that an HSP90 inhibitor, geldanamycin, inhibits HCV RNA replication (25, 26). We examined whether or not teprenone induced HSP90 in hepatoma cells and found that it did not (supporting information, Fig. S4).

In this study, we monitored the geranylgeranylated state of Rap1A as a marker using nongeranylgeranylated Rap1A-detectable anti-Rap1A antibody (sc-1482). The least expected result of this sensitive geranylgeranylation assay is that teprenone enhanced statins' inhibitory action against geranylgeranylation. It is not clear in this study as to why teprenone enhanced statins' inhibitory action on geranylgeranylation. One possibility is that teprenone may cause biosynthesis from FPP to cholesterol rather than to GGPP by an unknown mechanism. To clarify this point, further study will be needed. This new function of teprenone may contribute to not only the antiviral field but also other fields, including studies on osteoporosis and on various kinds of antitumours, because geranylgeranylation and farnesylation are targets of the reagent in these fields. For example, statins interfere with the production of GGPP and FPP, which is important in the activation of small G proteins, such as K-ras and the Rho family, and disrupt the growth of malignant cells.

Recently, two important findings have been reported. Firstly, El-Serag *et al.* (8) reported that statins are associated with a reduced risk of HCC. Secondly, Abraldes *et al.* (9) reported that statin lowers portal pressure in patients with cirrhosis. Therefore, as teprenone is a strong adjuvant to statin's inhibitory action against geranylgeranylation, it may further improve portal hypertension in cirrhosis and reduce the risk of HCC in combination with statins. Although teprenone alone possesses modest anti-HCV activity, it will play a significant role in combination with IFN and/or statins in the therapy to HCV-associated liver diseases as an adjuvant like ribavirin. As teprenone is available in clinical use with a low side effect, a clinical study using teprenone in combination with IFN-α and/or statins is now underway in our institution.

In conclusion, we have shown that the anti-ulcer agent teprenone inhibited HCV RNA replication and enhanced statins' inhibitory action against geranylgeranylation. This newly discovered function of teprenone may contribute to improve the treatment of HCV-associated liver diseases (CH C, cirrhosis and HCC) as an adjuvant to statins.

Acknowledgements

The authors would like to thank Atsumi Morishita, Takashi Nakamura and Midori Takeda for their technical assistance. This work was supported by grants-in-aid for a third-term comprehensive 10-year strategy for cancer control and for research on hepatitis from the Ministry of Health, Labor, and Welfare of Japan. K. A. and K. M. were supported by a Research Fellowship from the Japan Society for the Promotion of Science (JSPS) for Young Scientists.

References

1. Feld JJ, Hoofnagle JH. Mechanism of action of interferon and ribavirin in treatment of hepatitis C. *Nature* 2005; **436**: 967–72.
2. Ikeda M, Abe K, Dansako H, *et al.* Efficient replication of a full-length hepatitis C virus genome, strain O, in cell culture, and development of a luciferase reporter system. *Biochem Biophys Res Commun* 2005; **329**: 1350–9.
3. Ikeda M, Abe K, Yamada M, *et al.* Different anti-HCV profiles of statins and their potential for combination therapy with interferon. *Hepatology* 2006; **44**: 117–25.
4. Ikeda M, Kato N. Modulation of host metabolism as a target of new antivirals. *Adv Drug Deliv Rev* 2007; **59**: 1277–89.
5. Ikeda M, Kato N. Life style-related diseases of the digestive system: cell culture system for the screening of anti-hepatitis C virus HCV reagents: suppression of HCV replication by statins and synergistic action with interferon. *J Pharmacol Sci* 2007; **105**: 145–50.
6. Kim SS, Peng LF, Lin W, *et al.* A cell-based, high-throughput screen for small molecule regulators of hepatitis C virus replication. *Gastroenterology* 2007; **132**: 311–20.
7. Bader T, Fazili J, Madhoun M, *et al.* Fluvastatin inhibits hepatitis C replication in humans. *Am J Gastroenterol* 2008; **103**: 1383–9.
8. El-Serag HB, Johnson ML, Hachem C, Morgana RO. Statins are associated with a reduced risk of hepatocellular carcinoma in a large cohort of patients with diabetes. *Gastroenterology* 2009; **136**: 1601–8.
9. Abraldes JG, Albillos A, Banares R, *et al.* Simvastatin lowers portal pressure in patients with cirrhosis and portal hypertension: a randomized controlled trial. *Gastroenterology* 2009; **136**: 1651–8.

10. Kapadia SB, Chisari FV. Hepatitis C virus RNA replication is regulated by host geranylgeranylation and fatty acids. *Proc Natl Acad Sci USA* 2005; **102**: 2561–6.
11. Ye J, Wang C, Sumpter R Jr, *et al.* Disruption of hepatitis C virus RNA replication through inhibition of host protein geranylgeranylation. *Proc Natl Acad Sci USA* 2003; **100**: 15865–70.
12. Wang C, Gale M Jr, Keller BC, *et al.* Identification of FBL2 as a geranylgeranylated cellular protein required for hepatitis C virus RNA replication. *Mol Cell* 2005; **18**: 425–34.
13. Lindenbach BD, Evans MJ, Syder AJ, *et al.* Complete replication of hepatitis C virus in cell culture. *Science* 2005; **309**: 623–6.
14. Wakita T, Pietschmann T, Kato T, *et al.* Production of infectious hepatitis C virus in tissue culture from a cloned viral genome. *Nat Med* 2005; **11**: 791–6.
15. Zhong J, Gastaminza P, Cheng G, *et al.* Robust hepatitis C virus infection in vitro. *Proc Natl Acad Sci USA* 2005; **102**: 9294–9.
16. Nanke Y, Kotake S, Ninomiya T, *et al.* Geranylgeranylacetone inhibits formation and function of human osteoclasts and prevents bone loss in tail-suspended rats and ovariectomized rats. *Calcif Tissue Int* 2005; **77**: 376–85.
17. Kato N, Sugiyama K, Namba K, *et al.* Establishment of a hepatitis C virus subgenomic replicon derived from human hepatocytes infected in vitro. *Biochem Biophys Res Commun* 2003; **306**: 756–66.
18. Naka K, Ikeda M, Abe K, Dansako H, Kato N. Mizoribine inhibits hepatitis C virus RNA replication: effect of combination with interferon-alpha. *Biochem Biophys Res Commun* 2005; **330**: 871–9.
19. Dansako H, Naganuma A, Nakamura T, *et al.* Differential activation of interferon-inducible genes by hepatitis C virus core protein mediated by the interferon stimulated response element. *Virus Res* 2003; **97**: 17–30.
20. Ariumi Y, Kuroki M, Abe K, *et al.* DDX3 DEAD-box RNA helicase is required for hepatitis C virus RNA replication. *J Virol* 2007; **81**: 13922–6.
21. Hughes A, Rogers MJ, Idris AI, Crockett JC. A comparison between the effects of hydrophobic and hydrophilic statins on osteoclast function in vitro and ovariectomy-induced bone loss in vivo. *Calcif Tissue Int* 2007; **81**: 403–1.
22. Merrell MA, Wakchoure S, Lehenkari PP, Harris KW, Selander KS. Inhibition of the mevalonate pathway and activation of p38 MAP kinase are independently regulated by nitrogen-containing bisphosphonates in breast cancer cells. *Eur J Pharmacol* 2007; **570**: 27–37.
23. Ichikawa T, Nakao K, Nakata K, *et al.* Geranylgeranylacetone induces antiviral gene expression in human hepatoma cells. *Biochem Biophys Res Commun* 2001; **280**: 933–9.
24. Hirakawa T, Rokutan K, Nikawa T, Kishi K. Geranylgeranylacetone induces heat shock proteins in cultured guinea pig gastric mucosal cells and rat gastric mucosa. *Gastroenterology* 1996; **111**: 345–57.
25. Nakagawa S, Umehara T, Matsuda C, *et al.* Hsp90 inhibitors suppress HCV replication in replicon cells and humanized liver mice. *Biochem Biophys Res Commun* 2007; **353**: 882–8.
26. Okamoto T, Nishimura Y, Ichimura T, *et al.* Hepatitis C virus RNA replication is regulated by FKBP8 and Hsp90. *Embo J* 2006; **25**: 5015–25.

Supporting information

Additional supporting information may be found in the online version of this article:

Fig. S1. The effects of anti-ulcer agents on HCV RNA replication. (A) Cell proliferation assay. OR6 cells were treated with teprenone (0, 2.5, 5, 10, and 20 μg/ml), and the cells at 24, 48, and 72 hours after treatment were subjected to WST-1 cell proliferation assay. (B) Structures of ant-ulcer agents. (C-E) OR6 cells were treated with ecabet sodium (0, 2.5, 5, 10, 20 μg/ml) (C), sofalcon (0, 2.5, 5, 10, 20 μg/ml) (D), and gefarnate (0, 2.5, 5, 10, 20 μg/ml) (E) for 72 hours. Then the cells were subjected to luciferase assay (upper panel) and Western blot analysis using anti-core, and anti-β-actin antibodies (lower panel) as shown in Figure 1B.

Fig. S2. Teprenone didn't activate IFN signaling pathway. (A and B) Luciferase assays for 2'5'OAS and ISRE promoters. p2'5'OAS-luc (A) and pISRE-luc (B) transfected OR6c cells were treated with teprenone (0, 2.5, 5, and 10 μg/ml) or IFN-α (0, 2.5, 5, and 10 IU/ml) for 6 hours and then subjected to luciferase reporter assay. (C) Teprenone didn't activate STATs in OR6 cells. OR6 cells were treated with IFN-α (500 IU/ml), PTV (1.25 μM), and teprenone (20 μg/ml) for 0, 3, 6, and 12 hours. Then the cells were subjected to Western blot analysis using anti-pSTAT1 (Tyr701), anti-STAT1, anti-pSTAT2 (Tyr689), anti-core, and anti-β-actin antibodies.

Fig. S3. Teprenone treatment didn't cause positive feedback of HMG-CoA reductase (HMGCR). OR6c cells were treated with teprenone (20 μg/ml), PTV (10 μmol/L), or neither for 24 hours. The cells were subjected to RT-PCR (A) and real-time RT-quantitative PCR (B) using HMG-CoA reductase-specific primer set. H_2O was used as a negative control. GAPDH was used as an internal control.

Fig. S4. Teprenone didn't induce HSP90 or HSP70 in HuH-7 cells. OR6 cells were treated with teprenone (20 μg/ml) for 0, 3, 6, 12, 24, and 48 hours. Then the cells were subjected to Western blot analysis using anti-HSP90, anti-HSP70 anti-core, and anti-β-actin antibodies.

Please note: Wiley-Blackwell is not responsible for the content or functionality of any supporting materials supplied by the authors. Any queries (other than missing material) should be directed to the corresponding author for the article.

JOURNAL OF VIROLOGY, July 2011, p. 6882–6892 Vol. 85, No. 14
0022-538X/11/$12.00 doi:10.1128/JVI.02418-10

Hepatitis C Virus Hijacks P-Body and Stress Granule Components around Lipid Droplets▽

Yasuo Ariumi,[1,2]* Misao Kuroki,[1] Yukihiro Kushima,[3] Kanae Osugi,[4] Makoto Hijikata,[3] Masatoshi Maki,[4] Masanori Ikeda,[1] and Nobuyuki Kato[1]

Department of Tumor Virology, Okayama University Graduate School of Medicine, Dentistry, and Pharmaceutical Sciences, Okayama 700-8558, Japan[1]; Center for AIDS Research, Kumamoto University, Kumamoto 860-0811, Japan[2]; Department of Viral Oncology, Institute for Virus Research, Kyoto University, Kyoto 606-8507, Japan[3]; and Department of Applied Molecular Biosciences, Graduate School of Bioagricultural Sciences, Nagoya University, Nagoya 464-8601, Japan[4]

Received 19 November 2010/Accepted 21 April 2011

The microRNA miR-122 and DDX6/Rck/p54, a microRNA effector, have been implicated in hepatitis C virus (HCV) replication. In this study, we demonstrated for the first time that HCV-JFH1 infection disrupted processing (P)-body formation of the microRNA effectors DDX6, Lsm1, Xrn1, PATL1, and Ago2, but not the decapping enzyme DCP2, and dynamically redistributed these microRNA effectors to the HCV production factory around lipid droplets in HuH-7-derived RSc cells. Notably, HCV-JFH1 infection also redistributed the stress granule components GTPase-activating protein (SH3 domain)-binding protein 1 (G3BP1), ataxin-2 (ATX2), and poly(A)-binding protein 1 (PABP1) to the HCV production factory. In this regard, we found that the P-body formation of DDX6 began to be disrupted at 36 h postinfection. Consistently, G3BP1 transiently formed stress granules at 36 h postinfection. We then observed the ringlike formation of DDX6 or G3BP1 and colocalization with HCV core after 48 h postinfection, suggesting that the disruption of P-body formation and the hijacking of P-body and stress granule components occur at a late step of HCV infection. Furthermore, HCV infection could suppress stress granule formation in response to heat shock or treatment with arsenite. Importantly, we demonstrate that the accumulation of HCV RNA was significantly suppressed in DDX6, Lsm1, ATX2, and PABP1 knockdown cells after the inoculation of HCV-JFH1, suggesting that the P-body and the stress granule components are required for the HCV life cycle. Altogether, HCV seems to hijack the P-body and the stress granule components for HCV replication.

Hepatitis C virus (HCV) is the causative agent of chronic hepatitis, which progresses to liver cirrhosis and hepatocellular carcinoma. HCV is an enveloped virus with a positive single-stranded 9.6-kb RNA genome, which encodes a large polyprotein precursor of approximately 3,000 amino acid (aa) residues. This polyprotein is cleaved by a combination of the host and viral proteases into at least 10 proteins in the following order: core, envelope 1 (E1), E2, p7, nonstructural 2 (NS2), NS3, NS4A, NS4B, NS5A, and NS5B (12, 13, 21). The HCV core protein, a nucleocapsid, is targeted to lipid droplets (LDs), and the dimerization of the core protein by a disulfide bond is essential for the production of infectious virus (24). Recently, LDs have been found to be involved in an important cytoplasmic organelle for HCV production (26). Budding is an essential step in the life cycle of enveloped viruses. The endosomal sorting complex required for transport (ESCRT) system has been involved in such enveloped virus budding machineries, including that of HCV (5).

DEAD-box RNA helicases with ATP-dependent RNA-unwinding activities have been implicated in various RNA metabolic processes, including transcription, translation, RNA splicing, RNA transport, and RNA degradation (32). Previously, DDX3 was identified as an HCV core-interacting protein by yeast two-hybrid screening (25, 29, 43). Indeed, DDX3 is required for HCV RNA replication (3, 31). DDX6 (Rck/p54) is also required for HCV replication (16, 33). DDX6 interacts with an initiation factor, eukaryotic initiation factor 4E (eIF-4E), to repress the translational activity of mRNP (38). Furthermore, DDX6 regulates the activity of the decapping enzymes DCP1 and DCP2 and interacts directly with Argonaute-1 (Ago1) and Ago2 in the microRNA (miRNA)-induced silencing complex (miRISC) and is involved in RNA silencing. DDX6 localizes predominantly in the discrete cytoplasmic foci termed the processing (P) body. Thus, the P body seems to be an aggregate of translationally repressed mRNPs associated with the translation repression and mRNA decay machinery.

In addition to the P body, eukaryotic cells contain another type of RNA granule termed the stress granule (SG) (1, 6, 22, 30). SGs are aggregates of untranslating mRNAs in conjunction with a subset of translation initiation factors (eIF4E, eIF3, eIF4A, eIFG, and poly(A)-binding protein [PABP]), the 40S ribosomal subunits, and several RNA-binding proteins, including PABP, T cell intracellular antigen 1 (TIA-1), TIA-1-related protein (TIAR), and GTPase-activating protein (SH3 domain)-binding protein 1 (G3BP1). SGs regulate mRNA translation and decay as well as proteins involved in various aspects of mRNA metabolisms. SGs are cytoplasmic phase-dense structures that occur in eukaryotic cells exposed to various environmental stress, including heat, arsenite, viral infection, oxidative conditions, UV irradiation, and hypoxia. Impor-

* Corresponding author. Mailing address: Center for AIDS Research, Kumamoto University, 2-2-1 Honjo, Kumamoto 860-0811, Japan. Phone and fax: 81 96 373 6834. E-mail: ariumi@kumamoto-u.ac.jp.
▽ Published ahead of print on 4 May 2011.

tantly, several viruses target SGs and stress granule components for viral replication (10, 11, 34, 39). Recent studies suggest that SGs and the P body physically interact and that mRNAs may move between the two compartments (1, 6, 22, 28, 30).

miRNAs are a class of small noncoding RNA molecules ~21 to 22 nucleotides (nt) in length. miRNAs usually interact with 3′-untranslated regions (UTRs) of target mRNAs, leading to the downregulation of mRNA expression. Notably, the liver-specific and abundant miR-122 interacts with the 5′-UTR of the HCV RNA genome and facilitates HCV replication (15, 17, 19, 20, 31). Ago2 is at least required for the efficient miR-122 regulation of HCV RNA accumulation and translation (40). However, the molecular mechanism(s) for how DDX6 and miR-122 as well as DDX3 positively regulate HCV replication is not fully understood. Therefore, we investigated the potential role of P-body and stress granule components in HCV replication.

MATERIALS AND METHODS

Cell culture. 293FT cells were cultured in Dulbecco's modified Eagle's medium (DMEM; Invitrogen, Carlsbad, CA) supplemented with 10% fetal bovine serum (FBS). HuH-7-derived RSc cured cells, in which cell culture-generated HCV-JFH1 (JFH1 strain of genotype 2a) (37) could infect and effectively replicate, were cultured in DMEM with 10% FBS as described previously (3–5, 23).

Plasmid construction. To construct pcDNA3-FLAG-DDX6, a DNA fragment encoding DDX6 was amplified from total RNAs derived from RSc cells by reverse transcription (RT)-PCR using KOD-Plus DNA polymerase (Toyobo) and the following pairs of primers: 5′-CGGGATCCAAGATGAGCACGGCC AGAACAGAGAACCCTGTT-3′ (forward) and 5′-CCGCTCGAGTTAAGGT TTCTCATCTTCTACAGGCTCGCT-3′ (reverse). The obtained DNA fragments were subcloned into either BamHI-XhoI site of the pcDNA3-FLAG vector (2), and the nucleotide sequences were determined by BigDye termination cycle sequencing using an ABI Prism 310 genetic analyzer (Applied Biosystems, Foster City, CA).

RNA interference. The following small interfering RNAs (siRNAs) were used: human ATXN2/ATX2/ataxin-2 (siGENOME SMRT pool M-011772-01-005), human PABP1/PABPC1 (siGENOME SMRT pool M-019598-01-005), human Lsm1 (siGENOME SMRT pool M-005124-01-005), human Xrn1 (siGENOME SMRT pool M-013754-01-005), human G3BP1 (ON-TARGETplus SMRT pool L-012099-00-005), human PATL1 (siGENOME SMRT pool M-015591-00-005), and siGENOME nontargeting siRNA pool 1 (D-001206-13-05) (Dharmacon, Thermo Fisher Scientific, Waltham, MA), as a control. siRNAs (25 nM final concentration) were transiently transfected into RSc cells (3–5, 23) using Oligofectamine (Invitrogen) according to the manufacturer's instructions. Oligonucleotides with the following sense and antisense sequences were used for the cloning of short hairpin RNA (shRNA)-encoding sequences targeted to DDX6 (DDX6i) as well as the control nontargeting shRNA (shCon) in a lentiviral vector: 5′-GATCC CCGGAGGAACTAACTCTGAAGTTCAAGAGACTTCAGAGTTAGTTCCT CCTTTTTGGAAA-3′ (sense) and 5′-AGCTTTTCCAAAAAGGAGGAACTAA CTCTGAAGTCTCTTGAACTTCAGAGTTAGTTCCTCCGGG-3′ (antisense) for DDX6i and 5′-GATCCCCGAATCCAGAGGTAATCTACTTCAAGAGA GTAGATTACCTCTGGATTCTTTTTGGAAA-3′ (sense) and 5′-AGCTTTTC CAAAAAGAATCCAGAGGTAATCTACTCTCTTGAAGTAGATTACCTC TGGATTCGGG-3′ (antisense) for shCon. The oligonucleotides described above were annealed and subcloned into the BglII-HindIII site, downstream from an RNA polymerase III promoter of pSUPER (8), to generate pSUPER-DDX6i and pSUPER-shCon, respectively. To construct pLV-DDX6i and pLV-shCon, the BamHI-SalI fragments of the corresponding pSUPER plasmids were subcloned into the BamHI-SalI site of pRDI292, an HIV-1-derived self-inactivating lentiviral vector containing a puromycin resistance marker allowing for the selection of transduced cells (7). pLV-DDX3i, described previously (3), was used.

Lentiviral vector production. The vesicular stomatitis virus G protein (VSV-G)-pseudotyped HIV-1-based vector system was described previously (27, 44). The lentiviral vector particles were produced by the transient transfection of the second-generation packaging construct pCMV-ΔR8.91 (27, 44), the VSV-G-envelope-expressing plasmid pMDG2, as well as pRDI292 into 293FT cells with FuGene6 reagent (Roche Diagnostics, Mannheim, Germany).

HCV infection experiments. The supernatants were collected from cell culture-generated HCV-JFH1 (37)-infected RSc cells (3–5, 23) at 5 days postinfection and stored at −80°C after filtering through a 0.45-μm filter (Kurabo, Osaka, Japan) until use. For infection experiments with HCV-JFH1, RSc cells (1×10^5 cells/well) were plated onto 6-well plates and cultured for 24 h. We then infected the cells at a multiplicity of infection (MOI) of 1 or 4. The culture supernatants were collected at 24 h postinfection, and the levels of the core protein were determined by an enzyme-linked immunosorbent assay (ELISA) (Mitsubishi Kagaku Bio-Clinical Laboratories, Tokyo, Japan). Total RNA was also isolated from the infected cellular lysates by using an RNeasy minikit (Qiagen, Hilden, Germany) for analysis of intracellular HCV RNA. The infectivity of HCV-JFH1 in the culture supernatants was determined by a focus-forming assay at 48 h postinfection. HCV-JFH1-infected cells were detected by using anti-HCV core (CP-9 and CP-11 mixture).

Quantitative RT-PCR analysis. The quantitative RT-PCR analysis of HCV RNA was performed by real-time LightCycler PCR (Roche) as described previously (3–5, 14, 23). We used the following forward and reverse primer sets for the real-time LightCycler PCR: 5′-ATGAGTCATGTGGCAGTGGA-3′ (forward) and 5′-GCTGGCTGTACTTCCTCCAC-3′ (reverse) for DDX3, 5′-ATG AGCACGGCCAGAACAGA-3′ (forward) and 5′-TTGCTGTGTCTGTGTGC CCC-3′ (reverse) for DDX6, 5′-TGACGGGGTCACCCACACTG-3′ (forward) and 5′-AAGCTGTAGCCGCGCTCGGT-3′ (reverse) for β-actin, and 5′-AGA GCCATAGTGGTCTGCGG-3′ (forward) and 5′-CTTTCGCAACCCAACGC TAC-3′ (reverse) for HCV-JFH1.

Preparation of anti-PATL1 antibody. The anti-PATL1 antiserum was raised in rabbits using the glutathione *S*-transferase (GST)-fused PATL1 Ct (C-terminal region of PATL1, aa 450 to 770) as an antigen, and immunoglobulins were affinity purified by using the maltose-binding protein (MBP)-fused PATL1 Ct that was immobilized on an *N*-hydroxysuccinimide (NHS) column (GE Healthcare Bio-Sciences AB, Uppsala, Sweden).

Preparation of LDs. Lipid droplets (LDs) were prepared as described previously (26). Cells were pelleted by centrifugation at 1,500 rpm. The pellet was resuspended in hypotonic buffer (50 mM HEPES [pH 7.4], 1 mM EDTA, 2 mM $MgCl_2$) supplemented with a protease inhibitor cocktail (Nacalai Tesque, Kyoto, Japan) and was incubated for 10 min at 4°C. The suspension was homogenized with 30 strokes of a glass Dounce homogenizer using a tight-fitting pestle (Wheaton, Millville, NJ). A 1/10 volume of 10× isotonic buffer {0.2 M HEPES (pH 7.4), 1.2 M potassium acetate (KoAc), 40 mM magnesium acetate [$Mg(oAc)_2$], and 50 mM dithiothreitol (DTT)} was added to the homogenate. The nuclei were removed by centrifugation at 2,000 rpm for 10 min at 4°C. The supernatant was collected and centrifuged at 16,000 × *g* for 10 min at 4°C. The supernatant was mixed with an equal volume of 1.04 M sucrose in isotonic buffer (50 mM HEPES, 100 mM KCl, 2 mM $MgCl_2$, and protease inhibitor cocktail). The solution was set in a 13.2-ml Polyallomer centrifuge tube (Beckman Coulter, Brea, CA). One milliliter of isotonic buffer was loaded onto the sucrose mixture. The tube was centrifuged at 100,000 × *g* in an SW41Ti rotor (Beckman Coulter) for 1 h at 4°C. After the centrifugation, the LD fraction on the top of the gradient solution was recovered in phosphate-buffered saline (PBS). The collected LD fraction was used for Western blot analysis.

Western blot analysis. Cells were lysed in a buffer containing 50 mM Tris-HCl (pH 8.0), 150 mM NaCl, 4 mM EDTA, 1% Nonidet P-40, 0.1% sodium dodecyl sulfate (SDS), 1 mM DTT, and 1 mM phenylmethylsulfonyl fluoride. Supernatants from these lysates were subjected to SDS-polyacrylamide gel electrophoresis, followed by immunoblot analysis using anti-DDX3 (catalog no. 54257 [NT] and 5428 [IN]; Anaspec, San Jose, CA), anti-DDX6 (A300-460A; Bethyl Laboratories, Montgomery, TX), anti-adipose differentiation-related protein (ADFP; GTX110204; GeneTex, San Antonio, TX), anti-calnexin (NT; Stressgen, Ann Arbor, MI), anti-HCV core (CP-9 and CP-11; Institute of Immunology, Tokyo, Japan), anti-β-actin antibody (A5441; Sigma, St. Louis, MO), anti-ATX2/SCA2 antibody (A302-033A; Bethyl), anti-PABP (sc-32318 [10E10]; Santa Cruz Biotechnology, Santa Cruz, CA), anti-PABP (ab21060; Abcam, Cambridge, United Kingdom), anti-G3BP1 (611126; BD Transduction Laboratories, San Jose, CA), anti-LSM1 (LS-C97364, Life Span Biosciences, Seattle, WA), anti-HSP70 (610607; BD), anti-XRN1 (A300-443A; Bethyl), or anti-PATL1 antibody.

Immunofluorescence and confocal microscopic analysis. Cells were fixed in 3.6% formaldehyde in PBS, permeabilized in 0.1% NP-40 in PBS at room temperature, and incubated with anti-DDX3 antibody (54257 [NT] and 5428 [IN]; Anaspec), anti-DDX3X (LS-C64576; Life Span), anti-DDX6 (A300-460A; Bethyl), anti-HCV core (CP-9 and CP-11), anti-ATX2/SCA2 antibody (A302-033A; Bethyl), anti-ataxin-2 (611378; BD), anti-PABP (ab21060; Abcam), anti-G3BP1 (A302-033A; Bethyl), anti-LSM1 (LS-C97364; Life Span), anti-XRN1

(A300-443A; Bethyl), anti-Dcp2 (A302-597A; Bethyl), anti-human Ago2 (011-22033; Wako, Osaka, Japan), or anti-PATL1 antibody at a 1:300 dilution in PBS containing 3% bovine serum albumin (BSA) for 30 min at 37°C. The cells were then stained with fluorescein isothiocyanate (FITC)-conjugated anti-rabbit antibody (Jackson ImmunoResearch, West Grove, PA) at a 1:300 dilution in PBS containing BSA for 30 min at 37°C. Lipid droplets and nuclei were stained with borondipyrromethene (BODIPY) 493/503 (Molecular Probes, Invitrogen) and DAPI (4′,6-diamidino-2-phenylindole), respectively, for 15 min at room temperature. Following extensive washing in PBS, the cells were mounted onto slides using a mounting medium of 90% glycerin–10% PBS with 0.01% *p*-phenylenediamine added to reduce fading. Samples were viewed under a confocal laser scanning microscope (LSM510; Zeiss, Jena, Germany).

Statistical analysis. A statistical comparison of the infectivities of HCV in the culture supernatants between the knockdown cells and the control cells was performed by using the Student *t* test. *P* values of less than 0.05 were considered statistically significant. All error bars indicate standard deviations.

RESULTS

HCV infection hijacks the P-body components. To investigate the potential role of P-body components in the HCV life cycle, we first examined the alteration of the subcellular localization of DDX3 or DDX6 by HCV-JFH1 infection using confocal laser scanning microscopy as previously described (2), since both DDX3 and DDX6 were identified previously as P-body components (6). For this, we used HuH-7-derived RSc cells, in which cell culture-generated HCV-JFH1 (JFH1 strain of genotype 2a) (37) can infect and effectively replicate (3, 4, 23). HCV-JFH1-infected RSc cells at 60 h postinfection were stained with anti-HCV core antibody, anti-DDX3, and/or anti-DDX6. Lipid droplets (LDs) and nuclei were stained with BODIPY 493/503 and DAPI (4′,6-diamidino-2-phenylindole), respectively. Samples were viewed under a confocal laser scanning microscope. Although we observed that endogenous DDX3 localized in faint cytoplasmic foci in uninfected RSc cells, DDX3 relocalized, formed ringlike structures, and colocalized with the HCV core protein in response to HCV-JFH1 infection (Fig. 1A). On the other hand, endogenous DDX6 was localized in the evident cytoplasmic foci termed P bodies in the uninfected cells (Fig. 1A). DDX6 also relocalized, formed ringlike structures, and colocalized with the core protein in response to HCV-JFH1 infection (Fig. 1A). Although we failed to observe that most of the P bodies of DDX6 perfectly colocalized with DDX3 in uninfected RSc cells (Fig. 1B), we observed a few P bodies of DDX6 colocalized with DDX3 in the uninfected cells (Fig. 1B, arrowheads). Intriguingly, we found that endogenous DDX3 colocalized with endogenous DDX6 in HCV-JFH1-infected cells (Fig. 1B). To further confirm this finding, pHA-DDX3 (41) and pcDNA3-FLAG-DDX6 were cotransfected into 293FT cells. Consequently, we observed that hemagglutinin (HA)-DDX3 colocalized with FLAG-DDX6 in 293FT cells coexpressing HA-DDX3 and FLAG-DDX6 (Fig. 1B), suggesting cross talk of DDX3 with DDX6. Recently, LDs have been found to be involved in an important cytoplasmic organelle for HCV production (26). Indeed, both DDX3 and DDX6 were recruited around LDs in response to HCV infection, while these proteins did not colocalize with LDs in uninfected naïve RSc cells (Fig. 1C). Furthermore, both DDX3 and DDX6 accumulated in the LD fraction of the HCV-JFH1-infected RSc cells; however, we could not detect both proteins in the LD fraction from uninfected control cells (Fig. 1D), suggesting that DDX3 and DDX6 are recruited around LDs in response to HCV infection.

These results suggest that HCV-JFH1 infection disrupts P-body formation. Therefore, we further examined whether or not HCV-JFH1 disrupts the P-body formations of other microRNA effectors, including Ago2; the Sm-like protein Lsm1, which is a subunit of heptameric-ring Lsm1-7, involved in decapping; the 5′-to-3′ exonuclease Xrn1; the decapping activator PATL1; and the decapping enzyme DCP2 (6, 21, 30). As expected, HCV-JFH1 disrupted the P-body formations of Ago2, Lsm1, and Xrn1 as well as PATL1 (Fig. 2). Lsm1, Xrn1, or PATL1 relocalized, formed ringlike structures, and colocalized with the HCV core protein in response to HCV-JFH1 infection, whereas they were localized predominantly in P bodies in uninfected RSc cells (Fig. 2). In fact, we observed that DDX6 colocalized with Ago2, a P-body marker (Fig. 2). In contrast, HCV-JFH1 failed to disrupt the P-body formation of DCP2 (Fig. 2). Thus, these results suggest that HCV disrupts P-body formation through the hijacking of P-body components.

HCV hijacks stress granule components. Since Nonhoff et al. recently reported that DDX6 interacted with ataxin-2 (ATX2) (28), we examined the potential cross talk among DDX6, ATX2, and HCV. Although ATX2 and G3BP1, a well-known stress granule component (36), were dispersed in the cytoplasm at 37°C, both proteins formed discrete aggregates termed stress granules and colocalized with each other in response to heat shock at 43°C for 45 min, indicating that ATX2 is also stress granule component (Fig. 3A). We did not observe prominent colocalization between DDX6 and ATX2 at 37°C (Fig. 3B). In contrast, we found that DDX6 was recruited, juxtaposed, and partially colocalized with stress granules of ATX2 in response to heat shock at 43°C for 45 min in the uninfected RSc cells (Fig. 3B). Notably, ATX2 was recruited, formed the ring-like structures, and partially colocalized with DDX6 in response to HCV-JFH1 infection even at 37°C (Fig. 3B). Furthermore, we noticed that ATX2 was recruited around LDs in HCV-JFH1-infected cells at 72 h postinfection, while ATX2 did not colocalize with LDs in uninfected cells (Fig. 3C), suggesting the colocalization of ATX2 with the HCV core protein in infected cells. Indeed, ATX2 colocalized with the HCV core protein in HCV-JFH1-infected RSc cells at 37°C (Fig. 3D). Moreover, HCV-JFH1 infection induced the colocalization of the core protein with other stress granule components, G3BP1 or PABP1 as well as ATX2 (Fig. 4 and 5). To further confirm our findings, we examined the time course of the redistribution of DDX6 and G3BP1 after inoculation with HCV-JFH1. Consequently, we still detected the P-body formation of DDX6 and dispersed G3BP1 in the cytoplasm, and we did not observe a colocalization between the HCV core protein and DDX6 at 12 and 24 h postinfection (Fig. 4). In contrast, we found that the P-body formation of DDX6 began to be disrupted at 36 h postinfection (Fig. 4). Consistently, G3BP1 formed stress granules at 36 h postinfection (Fig. 4). We then noticed a ringlike formation of DDX6 or G3BP1 and colocalization with the HCV core protein after 48 h postinfection (Fig. 4), suggesting that the disruption of P-body formation and the hijacking of P-body and stress granule components occur in a late step of HCV infection.

We then examined whether or not HCV-JFH1 infection

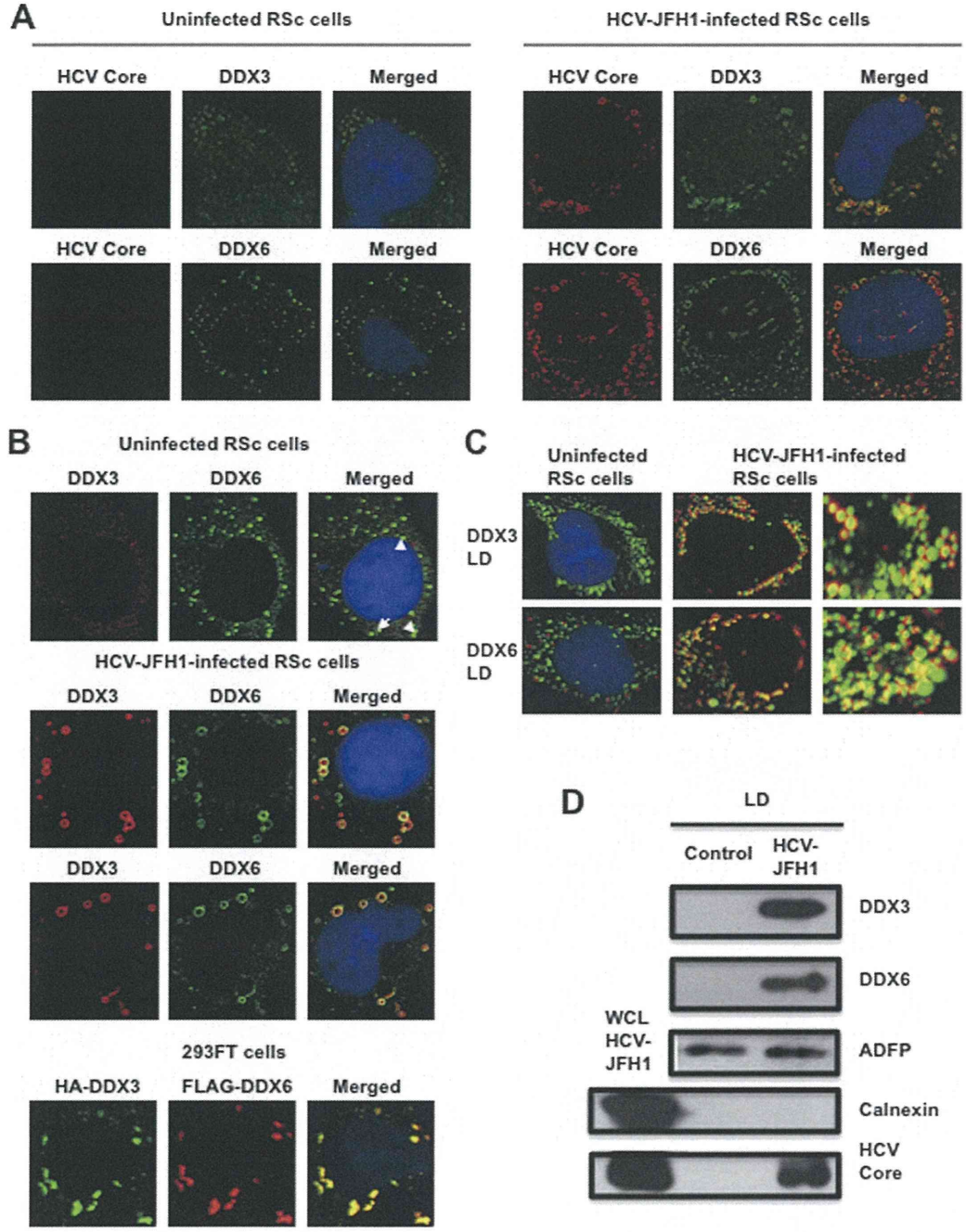

FIG. 1. Dynamic recruitment of DDX3 and DDX6 around lipid droplets (LDs) in response to HCV-JFH1 infection. (A) HCV-JFH1 disrupts the P-body formation of DDX6. Cells were fixed at 60 h postinfection and were then examined by confocal laser scanning microscopy. Cells were stained with anti-HCV core (CP-9 and CP-11 mixture) and either anti-DDX3 (54257 and 54258 mixture) or anti-DDX6 (A300-460A) antibody and then visualized with FITC (DDX3 or DDX6) or Cy3 (core). Images were visualized by using confocal laser scanning microscopy. The two-color overlay images are also exhibited (merged). Colocalization is shown in yellow. (B) HCV-JFH1 recruits DDX3 or DDX6 around LDs. Cells were stained with either anti-DDX3 or anti-DDX6 antibody and were then visualized with Cy3 (red). Lipid droplets and nuclei were stained with BODIPY 493/503 (green) and DAPI (blue), respectively. A high-magnification image is also shown. (C) Colocalization of DDX3 with DDX6. HCV-JFH1-infected RSc cells at 60 h postinfection were stained with anti-DDX3X (LS-C64576) and anti-DDX6 (A300-460A) antibodies. 293FT cells cotransfected with 100 ng of pcDNA3-FLAG-DDX6 and 100 ng of pHA-DDX3 (41) were stained with anti-FLAG-Cy3 and anti-HA-FITC antibodies (Sigma). (D) Association of DDX3 and DDX6 with LDs in response to HCV-JFH1 infection. The LD fraction and whole-cell lysates (WCL) were collected from uninfected RSc cells (control) or HCV-JFH1-infected RSc cells at 5 days postinfection. The results of Western blot analyses of DDX3, DDX6, and the HCV core protein as well as the LD marker ADFP and the endoplasmic reticulum (ER) marker calnexin in the LD fraction are shown.

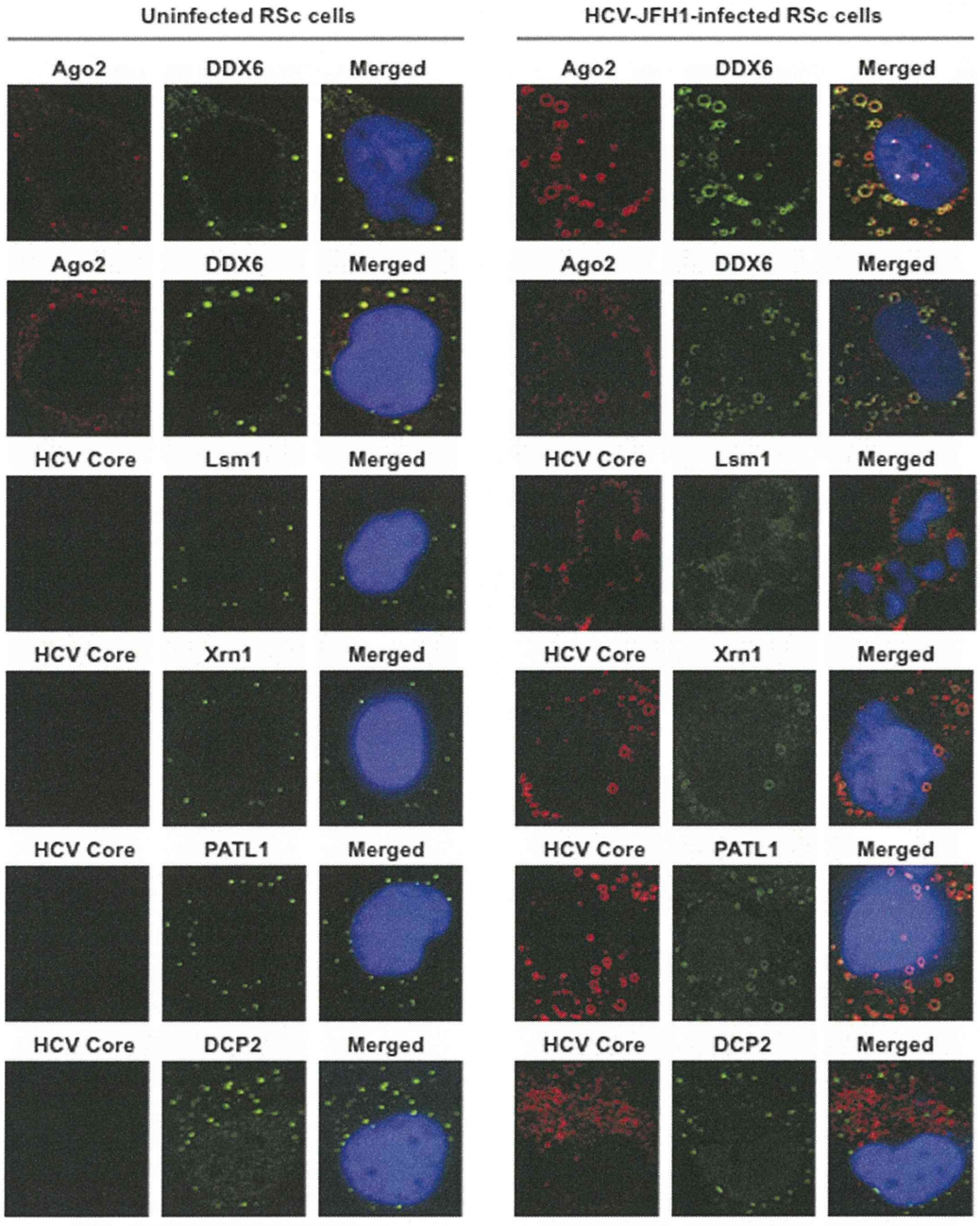

FIG. 2. HCV disrupts the P-body formation of microRNA effectors. Uninfected RSc cells and HCV-JFH1-infected RSc cells at 72 h postinfection were stained with anti-human AGO2 (011-22033) and anti-DDX6 (A300-460A) antibodies. The cells were also stained with anti-HCV core and anti-Lsm1 (LS-C97364), anti-Xrn1 (A300-443A), anti-PATL1, or anti-DCP2 (A302-597A) antibodies and were examined by confocal laser scanning microscopy.

could affect the stress granule formation of G3BP1, ATX2, or PABP1 in response to heat shock or treatment with arsenite. These stress granule components dispersed in the cytoplasm at 37°C, whereas these proteins formed stress granules in response to heat shock at 43°C for 45 min or treatment with 0.5 mM arsenite for 30 min (Fig. 5). In contrast, stress granules were not formed in HCV-JFH1-infected cells at 72 h postinfection in response to heat shock at 43°C for 45 min (Fig. 5), suggesting that HCV-JFH1 infection suppresses stress granule formation in response to heat shock or treatment with arsenite. Intriguingly, G3BP1, ATX2, or PABP1 still colocalized with the HCV core protein even under the above-described stress conditions (Fig. 5). Furthermore, Western blot analysis of cell lysates of uninfected or HCV-JFH1-infected cells at 72 h postinfection showed similar protein expression levels of ATX2, PABP1, HSP70, DDX3, DDX6, and Lsm1 but not G3BP1 (Fig. 6), suggesting that HCV-JFH1 infection does not affect host mRNA translation.

P-body and stress granule components are required for HCV replication. Finally, we investigated the potential role of

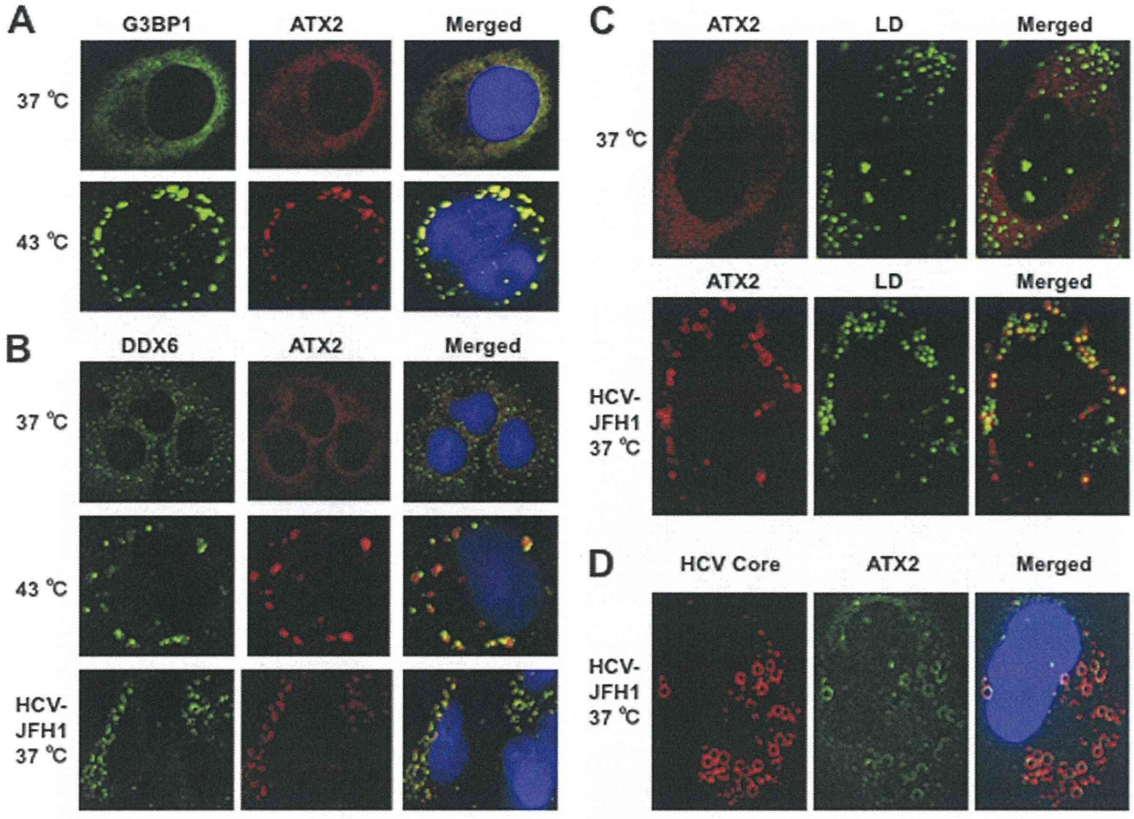

FIG. 3. Dynamic redistribution of ataxin-2 (ATX2) around LDs in response to HCV-JFH1 infection. (A) ATX2 is a stress granule component. RSc cells were incubated at 37°C or 43°C for 45 min. Cells were stained with anti-G3BP1 (A302-033A) and anti-ATX2 (A93520) antibodies and were examined by confocal laser scanning microscopy. (B) Dynamic redistribution of DDX6 and ATX2 in response to heat shock or HCV infection. RSc cells after heat shock at 43°C for 45 min or 72 h after inoculation with HCV-JFH1 were stained with anti-DDX6 and anti-ATX2 (A93520) antibodies. (C) HCV relocalizes ataxin-2 to LDs. HCV-JFH1-infected RSc cells at 72 h postinfection were stained with anti-ATX2 (A93520) antibody and BODIPY 493/503. (D) ATX2 colocalizes with the HCV core protein. HCV-JFH1-infected RSc cells at 72 h postinfection were stained with anti-ATX2/SCA2 (A301-118A) and anti-HCV core antibodies.

P-body and stress granule components in the HCV life cycle. We first used lentiviral vector-mediated RNA interference to stably knock down DDX6 as well as DDX3 in RSc cells. We used puromycin-resistant pooled cells 10 days after lentiviral transduction in all experiments. Real-time LightCycler RT-PCR analysis of DDX3 or DDX6 demonstrated a very effective knockdown of DDX3 or DDX6 in RSc cells transduced with lentiviral vectors expressing the corresponding shRNAs (Fig. 7A). Importantly, shRNAs did not affect cell viabilities (data not shown). We next examined the levels of HCV core and the infectivity of HCV in the culture supernatants as well as the level of intracellular HCV RNA in these knockdown cells 24 h after HCV-JFH1 infection at an MOI of 4. The results showed that the accumulation of HCV RNA was significantly suppressed in DDX3 or DDX6 knockdown cells (Fig. 7B). In this context, the release of the HCV core protein and the infectivity of HCV in the culture supernatants were also significantly suppressed in these knockdown cells (Fig. 7C and D). This finding suggested that DDX6 is required for HCV replication, like DDX3. To further examine the potential role of other P-body and stress granule components in HCV replication, we used RSc cells transiently transfected with a pool of siRNAs specific for ATX2, PABP1, Lsm1, Xrn1, G3BP1, and PATL1 as well as a pool of control siRNAs (siCon) following HCV-JFH1 infection. In spite of the very effective knockdown of each component (Fig. 7E), the siRNAs used in these experiments did not affect cell viabilities (data not shown). Consequently, the accumulation of HCV RNA was significantly suppressed in ATX2, PABP1, or Lsm1 knockdown cells (Fig. 7F), indicting that ATX2, PABP1, and Lsm1 are required for HCV replication. In contrast, the level of HCV RNA was not affected in Xrn1 knockdown cells (Fig. 7F), suggesting that Xrn1 is unrelated to HCV replication. Furthermore, we observed a moderate effect of siG3BP1 and siPATL1 on HCV RNA replication (Fig. 7F). Altogether, HCV seems to hijack the P-body and stress granule components around LDs for HCV replication.

DISCUSSION

So far, the P body and stress granules have been implicated in mRNA translation, RNA silencing, and RNA degradation as well as viral infection (1, 6, 22, 30). Host factors within the P body and stress granules can enhance or limit viral infection, and some viral RNAs and proteins accumulate in the P body and/or stress granules. Indeed, the microRNA effectors DDX6, GW182, Lsm1, and Xrn1 negatively regulate HIV-1 gene expression by preventing the association of viral mRNA

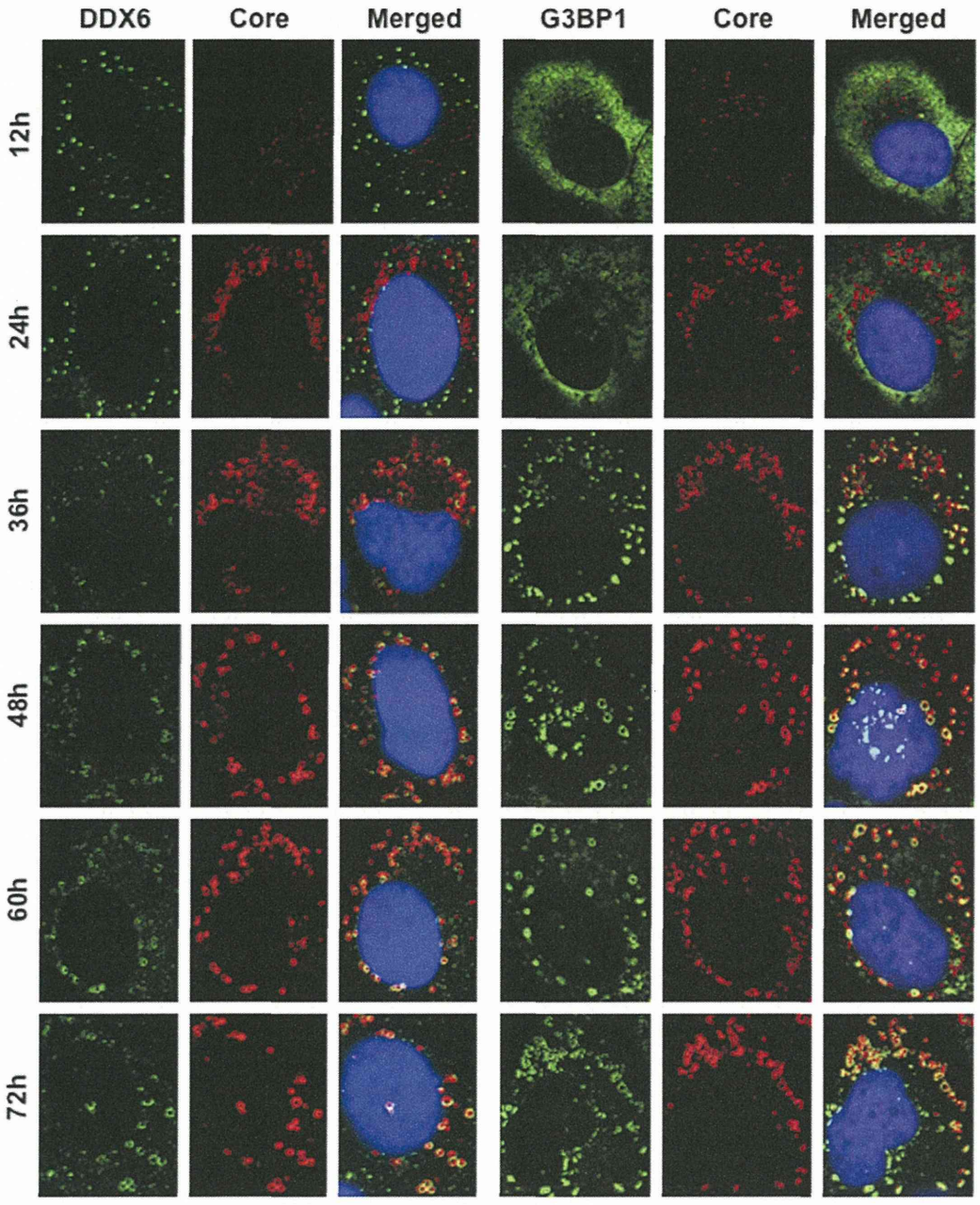

FIG. 4. Dynamic redistribution of DDX6 and G3BP1 in response to HCV-JFH1 infection. RSc cells at the indicated times (hours) after inoculation with HCV-JFH1 were stained with anti-HCV core and either anti-DDX6 (A300-460A) or anti-G3BP1 (A302-033A) antibodies.

with polysomes (9). In contrast, miRNA effectors such as DDX6, Lsm1, PatL1, and Ago2 positively regulate HCV replication (Fig. 7B and F) (16, 31, 33). We have also found that DDX3 and DDX6 are required for HCV RNA replication (3) (Fig. 7B) and that DDX3 colocalized with DDX6 in HCV-JFH1-infected RSc cells (Fig. 1B), suggesting that DDX3 comodulates the DDX6 function in HCV RNA replication. In this regard, the liver-specific miR-122 interacts with the 5′-UTR of the HCV RNA genome and positively regulates HCV replication (15, 17, 19, 20, 31). Since miRNAs usually interact with DDX6 and Ago2 in miRISC and are involved in RNA silencing, DDX6 and Ago2 may be required for miR-122-dependent HCV replication. Indeed, quite recently, a study showed that Ago2 is required for miR-122-dependent HCV RNA replication and translation (40). However, little is known regarding how miR-122 and DDX6 positively regulate HCV replication. Accordingly, we have shown that these miRNA effectors, including DDX6, Lsm1, Xrn1, and Ago2, accumulated around LDs and the HCV production factory and colocalized with the HCV core protein in response to HCV infection (Fig. 1 and 2). However, the decapping enzyme DCP2 did not accumulate and colocalize with the core protein (Fig. 2). Consistent with this finding, Scheller et al. reported previously that the depletion of DCP2 by siRNA did not affect HCV